ELECTRONIC SIGNAL PROCESSING TECHNIQUES

◄◄◄◄◄◄◄ **NONDESTRUCTIVE TESTING** ◄◄◄◄◄◄◄

PHASE III

FINAL REPORT

JANUARY, 1972

Details of illustrations in this document may be better studied on microfiche

D D C

RECEIVED

MAR 22 1972

B

THE ***BOEING*** COMPANY

SEATTLE WASHINGTON

DOCUMENT CONTROL DATA - R&D

(Security classification of title, body of abstract and indexing annotation must be entered when the overall report is classified).

1. ORIGINATING ACTIVITY (Corporate author)	2a. REPORT SECURITY CLASSIFICATION
The Boeing Company Aerospace Group Seattle, Washington 98124	Unclassified
	2b. GROUP

3. REPORT TITLE

Electronic Signal Processing Techniques Phase III– Nondestructive Testing

4. DESCRIPTIVE NOTES (Types of report and inclusive dates)

Final Report   15 December 1970 to 15 December 1971

5. AUTHORS (First name, middle initial, last name)

James C. Kennedy

Wayne E. Woodmansee

6. REPORT DATE	7a. TOTAL NO. OF PAGES	7b. NO. OF REFS
January 1972	73	6

8a. CONTRACT OR GRANT NO. DAAA 25-69-C0206	9a. ORIGINATOR'S REPORT NUMBERS
b. Project No. DA-W2-Z1246-F1-F6	The Boeing Company Report D180-10589-3
c. AMCMS Code 5910.21.202891	9b. OTHER REPORT NO(S) (Any other numbers that may be assigned this report)
d. ARPA Order No. 1246	

10. DISTRIBUTION STATEMENT

Distribution of this document is unlimited.

11. SUPPLEMENTARY NOTES	12. SPONSORING MILITARY ACTIVITY
	Advanced Research Projects Agency (ARPA) Washington, D. C. Frankford Arsenal, Philadelphia, Pa.

13. ABSTRACT

Correlation methods have been used to reduce surface roughness noise in eddy current and ultrasonic flaw detection systems. Titanium plates containing artificial flaws in the form of small drill holes and EDM slots have been ultrasonically inspected using multi-transducer techniques. It has been shown that cross-correlations formed between the various signals available significantly reduce the limiting background noise. A steel plate containing EDM slots has been inspected with an eddy current probe which produces four separate flaw detection signals. It has been shown that a quadruple product formed from these four signals reduces the background noise level. Initial tests indicate that coherent optical processing techniques are not likely to significantly enhance the clarity of marginal flaw signals on X-ray radiographs.

14.	KEY WORDS	LINK A		LINK B		LINK C	
		ROLE	WT	ROLE	WT	ROLE	2 T
	Data Analysis						
	Pattern Recognition						
	Digital Computer						
	Diagnostic Equipment						
	Flaw Detection						
	Acoustic Analysis						
	Statistical Analysis						
	Signature Analysis						
	Materials Evaluation						
	Optical Signal Processing						
	Correlation						
	Eddy Current						
	Ultrasonics						
	Nondestructive Testing						
	Signal Processing						
	Cross Correlation						
	Noise						

ELECTRONIC SIGNAL PROCESSING TECHNIQUES
PHASE III - NONDESTRUCTIVE TESTING

by

JAMES C. KENNEDY

and

WAYNE E. WOODMANSEE

Final Report
15 December 1970 to 15 December 1971

Contract Number DAAA 25-69-C0206

The Boeing Company
Seattle, Washington 98124

January 1972

FOREWORD

This report was prepared by The Boeing Company, Aerospace Group, Seattle, Washington under Contract DAAA 25-69-C0206 and covers the work performed between December 1970 and December 1971. This is the final report for Phase III of Electronic Signal Processing Techniques. Phase I was conducted between October 1968 and July 1969, and Phase II was conducted between October 1969 and October 1970.

The program was sponsored by the Advanced Research Projects Agency of the Department of Defense under ARPA Order 1246, Program Element Code G1101D. The program was administered under the direction of the Frankford Arsenal by Mr. Eugene Roffman.

The research was conducted at The Boeing Company, Kent Space Center Materials and Processes Laboratory. Mr. Eugene E. Bauer was the Program Manager, Dr. Wayne E. Woodmansee was the Technical Leader, and Mr. James C. Kennedy was the Principal Investigator.

ABSTRACT

Correlation methods have been used to reduce surface roughness noise in eddy current and ultrasonic flaw detection systems. Titanium plates containing artificial flaws in the form of small drill holes and EDM slots have been ultrasonically inspected using multi-transducer techniques. It has been shown that cross-correlations formed between the various signals available significantly reduce the limiting background noise. A steel plate containing EDM slots has been inspected with an eddy current probe which produces four separate flaw detection signals. It has been shown that a quadruple product formed from these four signals reduces the background noise level. Initial tests indicate that coherent optical processing techniques are not likely to significantly enhance the clarity of marginal flaw signals on X-ray radiographs.

TABLE OF CONTENTS

LIST OF ILLUSTRATIONS

INTRODUCTION

This is the final report covering a three year study for the Advanced Research
Projects Agency on the application of electronic signal processing techniques
to nondestructive testing. This report covers, in detail, the work of the last
twelve months and contains a review summary of the entire three year project.
During the first two years a number of different experiments were performed in-
volving the application of signal processing techniques to ultrasonic and eddy
current systems. The experiments involved noise reduction, recording, display,
and instrumentation development. Particular attention has been directed to the
reduction of surface roughness noise in both ultrasonic and eddy current systems.
Noise of this kind is not easily removed and frequently affects sensitivity.
Attempts to reduce surface roughness noise have led in the final year of activity
to the examination of multi-transducer and multi-coil systems. The cross corre-
lation of the various signals produced in such systems has in several cases produced
a significant reduction in background noise. An interesting aspect of this work is
the fact that improvements have been made in both ultrasonic and eddy current
systems using the same noise reduction principle. The details of these experiments
appear in the following pages.

DISCUSSION

CORRELATION METHODS IN ULTRASONIC WELD INSPECTION

Theory

Present ultrasonic weld inspection systems are limited in sensitivity by background noise due to the scattering of sound from surface irregularities and from the granular structure of the material. Even when the surface roughness and grain structure of a part are acceptable from a metallurgical standpoint one frequently obtains ultrasonic indications from these conditions which exceed the indications obtained from small cracks. The scattering of the ultrasound by surface roughness can be reduced by grinding or machining but some surface irregularities always remain. There is little that can be done about the granularity of a material except for the avoidance of high ultrasonic frequencies. Of course, if one works at frequencies much below a megacycle resolution is severely degraded.

The noise due to surface irregularities and grain scattering is readily visible in the CRT display of the pulsed ultrasonic signals. For a fixed transducer position, it consists of a stable pattern of irregular peaks[1]. It is important to note that the noise is not random in the usual sense. The noise signal is identical for each successive ultrasonic pulse and consequently a well defined pattern appears on the screen. Furthermore, although the pattern changes in a complicated manner for small changes in position of the transducer, the pattern will reproduce in detail if the transducer is carefully returned to its original position. The noise cannot be effectively reduced by conventional signal averaging procedures.

In the case of random noise, such as that which comes from amplifiers at high gain, successive signal pulses occur in different background noise patterns. This effect can be readily observed in a series of single sweep exposures taken from the CRT display. It is this basic feature which allows the signal to noise improvements to be made. In signal averagers the improvements are accomplished by the addition of signals from a large number of successive pulses. The noise, which tends to be negative as often as it is positive, averages to zero. The desired signal, which is always of the same size and polarity, is retained.

In the present work techniques were developed for producing flaw signals immersed in various background noise patterns, and signal to noise improvement was accomplished by multiplication of the patterns. The multiplication is performed on the gated video, which is an essentially DC signal. The ultrasonic transducers are set up for the inspection of the weld and the electronic gate is set to receive pulses from the region of the weld. As the transducer scans along the length of the weld, a signal is generated at the gate output which can be plotted on an XY pen recorder. Figure 11 is a typical data curve. The data contains flaw signals and an irregular noise background. Proper positioning of the transducers allows the production of several sets of data of this kind, each with a different background noise pattern.

Figures 12 and 13 are examples. Multiplication of these patterns produces significant improvements in signal to noise ratio. A triple product curve appears in Figure 15. It should be noted that, apart from the fact that no integration is used, the individual products are like a cross-correlation with zero time shift between the signals.

Initial correlations were made by inspecting a weld line from both sides, recording the results on an XY plotter, and performing point by point multiplication with a desk calculator. Transducer configurations were developed which would allow the collection of several different sets of data from the same side of the weld. Three of the sets were selected for analysis. They were recorded on magnetic tape and multiplication was performed on playback.

Finally, ultrasonic correlations were performed in real time. Five transducers were set up for the inspection of the same weld volume and were caused to scan as a unit along the length of the weld. A number of signals were available for multiplication, both pulse echo and pitch-catch. Three were selected for multiplication and a real time triple product was formed. The details appear in the sections to follow.

MULTIPLICATION OF TAPE RECORDED ULTRASONIC DATA

Specimen

The specimen is shown in Figure 1. This specimen was inspected as if it contained a weld seam with possible flaws. It is a quarter inch titanium plate one foot on a side. The specimen contains six artificial flaws in the form of drill holes and EDM slots. Dimensions are shown in the diagram. The line along which the holes and slots are located was taken to be the weld line.

Equipment and Procedure

The plate shown in Figure 1 was initially inspected using the pulse-echo shear wave immersion technique. A Sperry UM 721 Reflectoscope was used as pulser receiver. The inspection was performed at 5 MHz using a 1/2 inch diameter Automation Industries transducer. A closeup of the transducer and holder is shown in Figure 2. The transducer is firmly held in an aluminum block. A bolt has been used to fasten the block to a small vertically held aluminum plate. The block is free to rotate so that the angle between the sound beam and the normal to the surface of the test part can be adjusted.

The aluminum plate is adhesively bonded to a small but strong ferrite permanent magnet which forms the base of the transducer holder. Figure 3 shows the transducer mounted in position for inspecting the titanium plate. The transducer holder is magnetically attached to a steel plate which is part of the scanning unit. A piece of Teflon tape placed on the bottom of the ferrite magnet allows the transducer to be
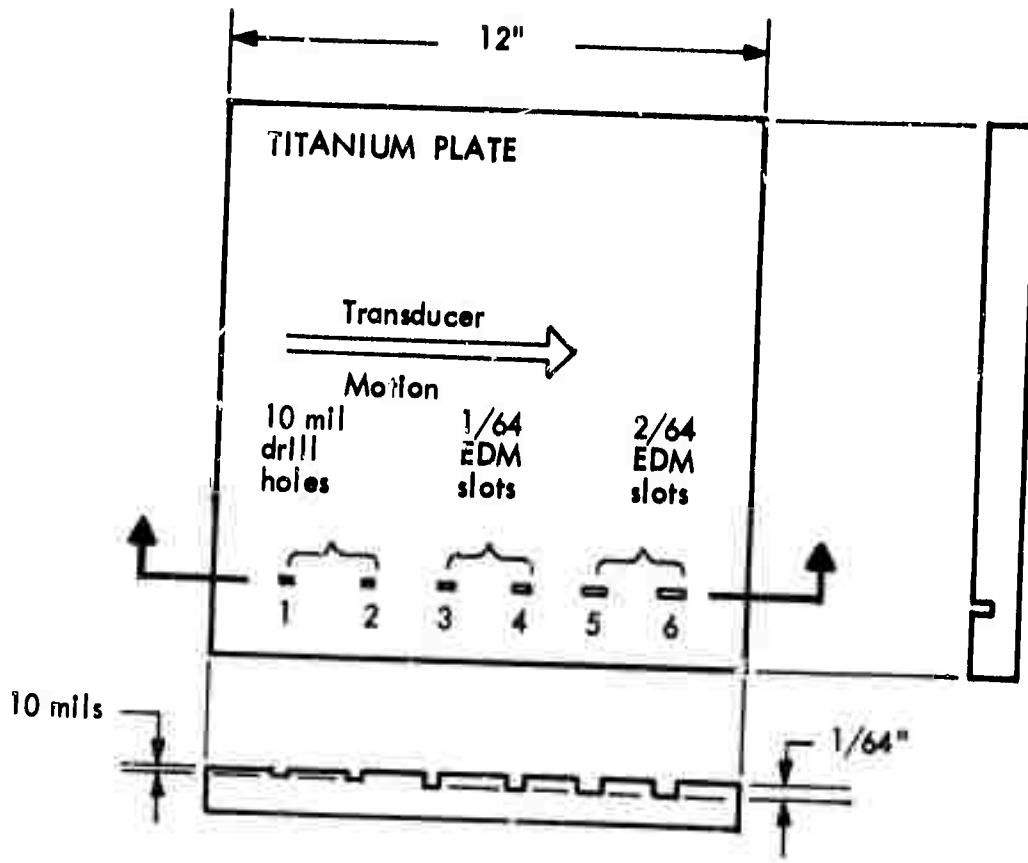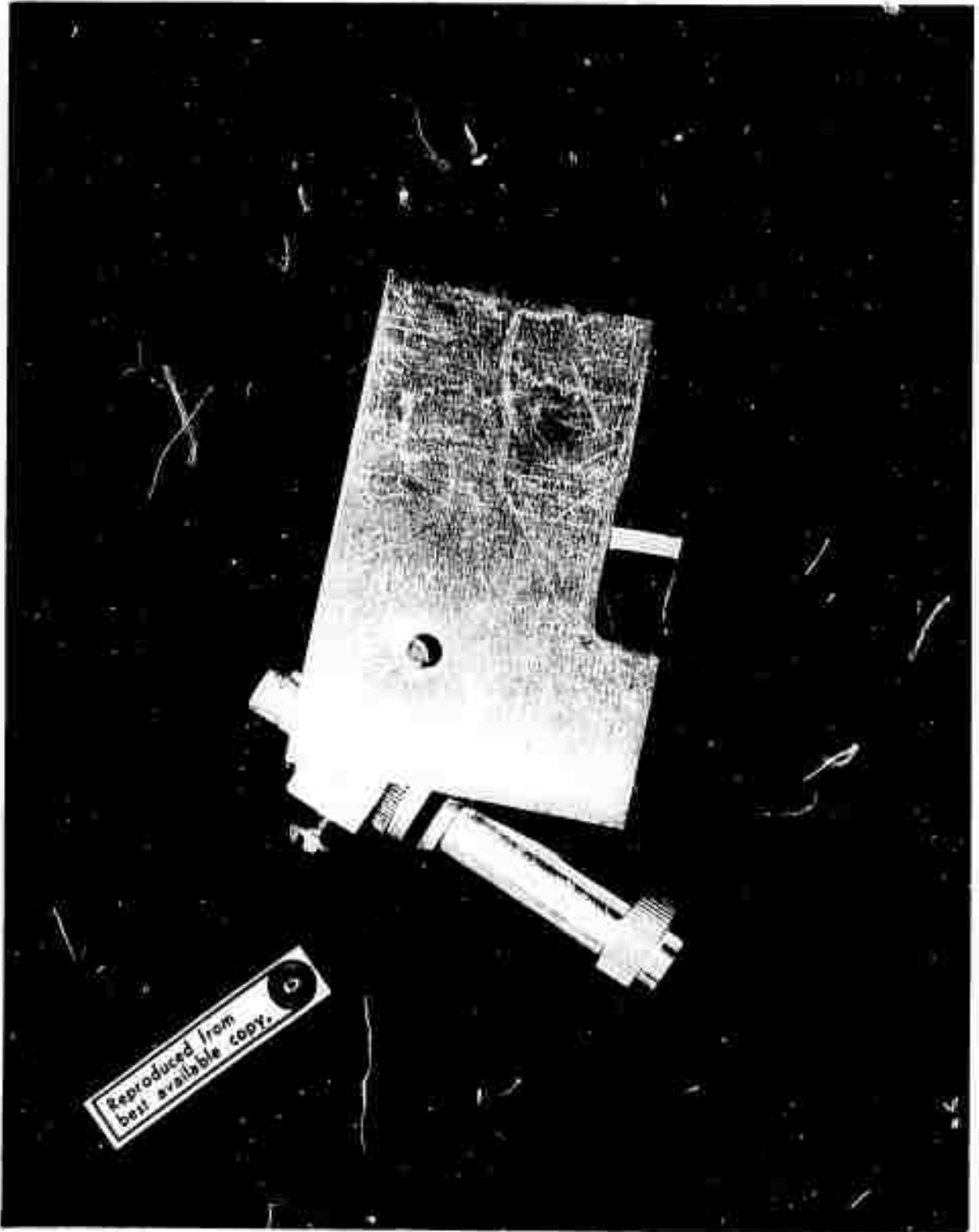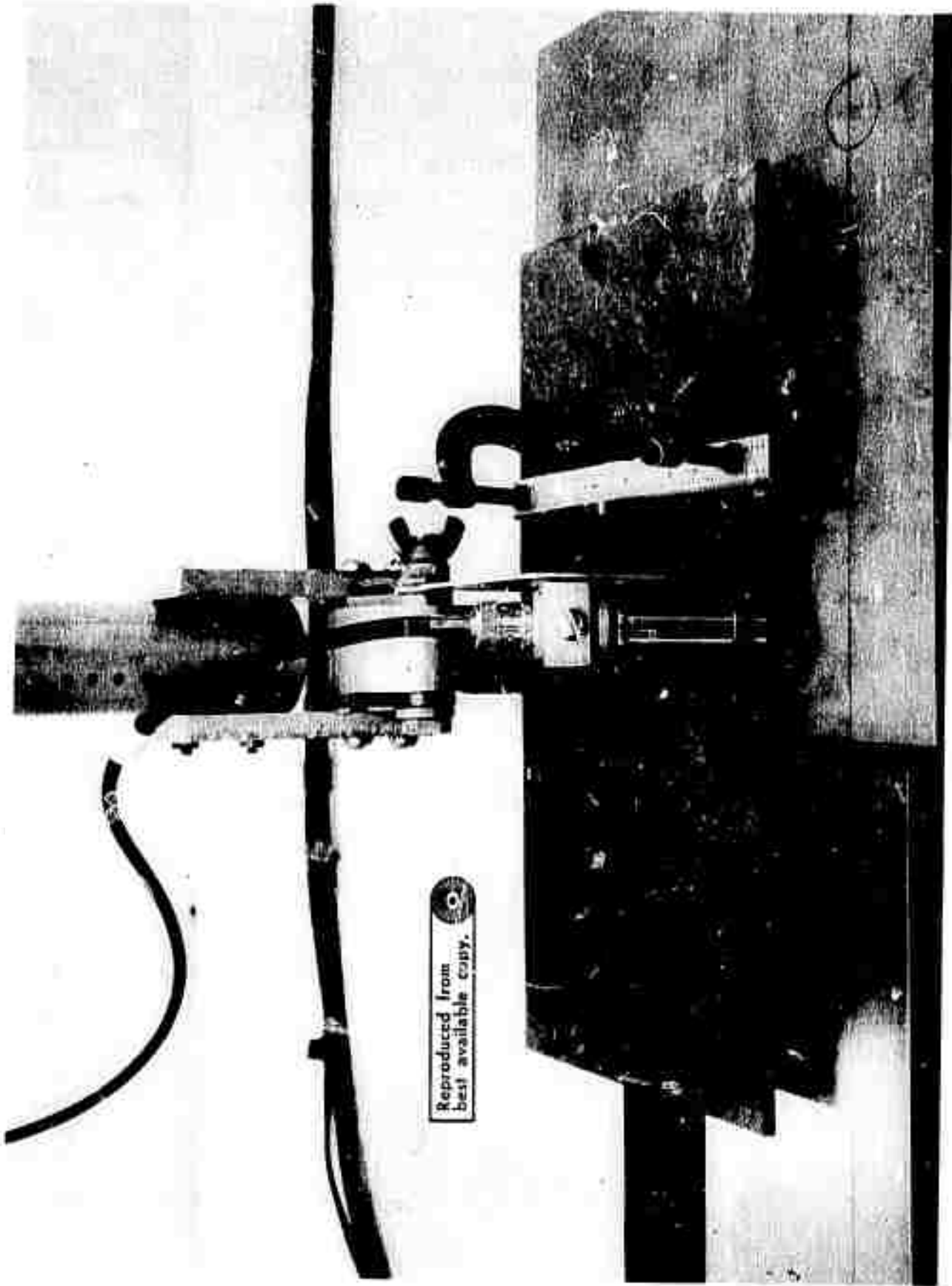
FIGURE 1   TEST SPECIMEN

FIGURE 2 TRANSDUCER HOLDER

FIGURE 3   CONVENTIONAL TRANSDUCER CONFIGURATION

6

easily moved to any desired location or angle. During inspection the entire assemblage moves along the length of the weld. A voltage indicating the position of the transducer is fed into the X axis of a Moseley 7000 recorder. The Sperry gate output is connected to the Y axis. Typical weld scan data can be seen in Figure 11.

The artificial flaws in the specimen used are all easily visible if the transducer is adjusted so that the sound path makes a small angle with the normal to the test part (eg. $\phi = 15°$ in Figure 4). In such a case, sound will be strongly reflected from the corner formed by the flat surface of the specimen and the face of the EDM slot or drill hole in question. In order to obtain an electronic signal more representative of a small totally interior crack, 21 degrees was selected as a value for ϕ. Under these conditions a 48 degree shear wave is set up in the part, and the smallest flaw indications have a signal to noise ratio of 1 to 1 or less.

Procedures were examined for obtaining several different sets of data from the same slice of "weld". It was desired that each set contain similar flaw indications but different background noise patterns. Initial correlations were obtained through point by point multiplication of data taken from the two sides of the weld line. The geometry for the collection of data from both sides of the weld can be seen in Figures 4a and 4b. However, as Figures 4c and 4d indicate this method is reliable for vertical flaws only. Another procedure is to examine the weld from the position shown in Figure 5. For this case we have observed a change in the fine structure of the noise but many of the larger noise peaks are the same as those obtained in the conventional configuration. A more successful procedure involves the use of the double transducer arrangement shown in Figure 6 and depicted more graphically in Figure 7. If the transducers are carefully located, this arrangement produces strong flaw signals immersed in a background noise pattern totally different from that obtained in the conventional configuration. Moreover, several different background noise patterns can be produced by selecting several different values for the angle θ. Figure 8 shows the two transducers mounted on the scanner with an included angle 2θ equal to 20 degrees. The recording and electronic gating procedures were the same for this case as they were for the single transducer configuration. Typical data for the dual transducer case can be seen in Figure 12.

One can envision the direction of the sound path as being defined by the angles ϕ, Figure 4, and θ, Figure 6. A major benefit of the transducer positioning fixture used in this work is that it provides convenient, independent adjustment of these two angles. For the data presented here both transducers of a given pair were set at $\phi = 21$ degrees. The angle θ was found to be more or less arbitrary. Angles less than 10 degrees are difficult because the transducers come into physical contact with one another. In data taken to date angles greater than 80 degrees have exhibited poor flaw sensitivity. Data I presented in this report for θ values of 20 and 30 degrees. The single transducer conventional pulse echo configuration can be though of as the $\theta = 0$ configuration.

7
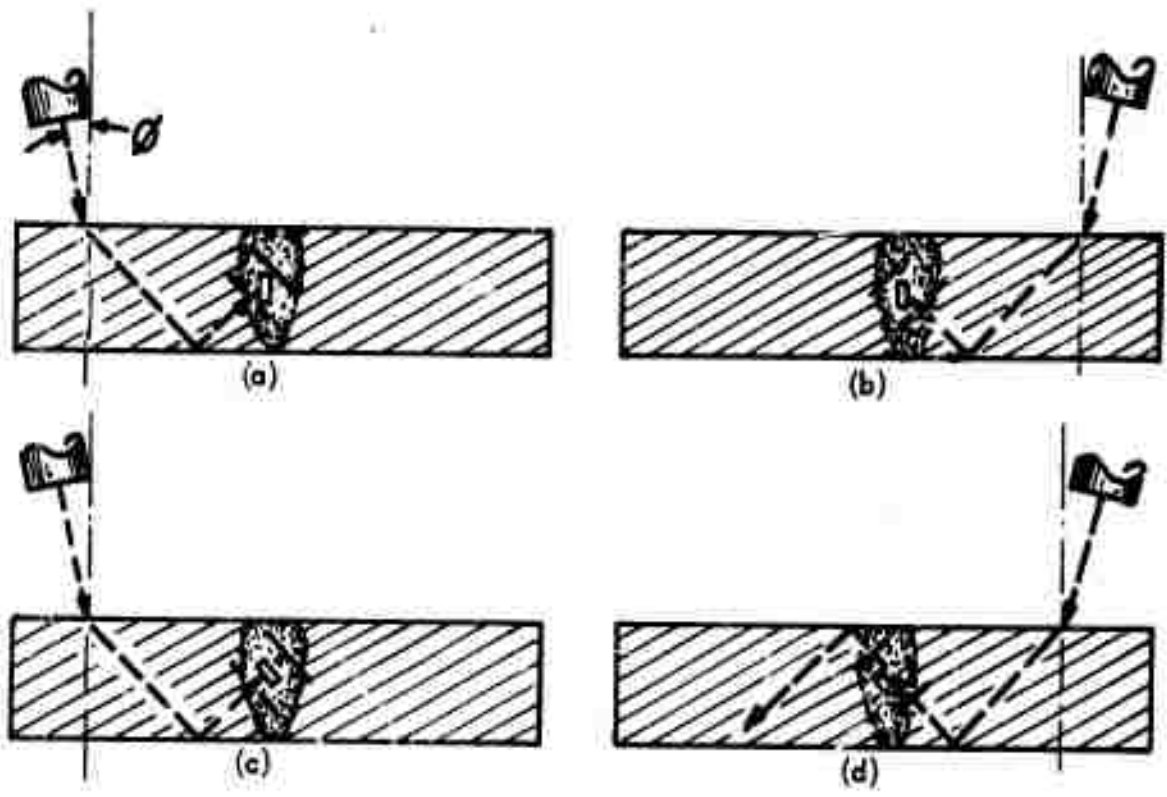
FIGURE 4   INSPECTION OF WELD FROM BOTH SIDES
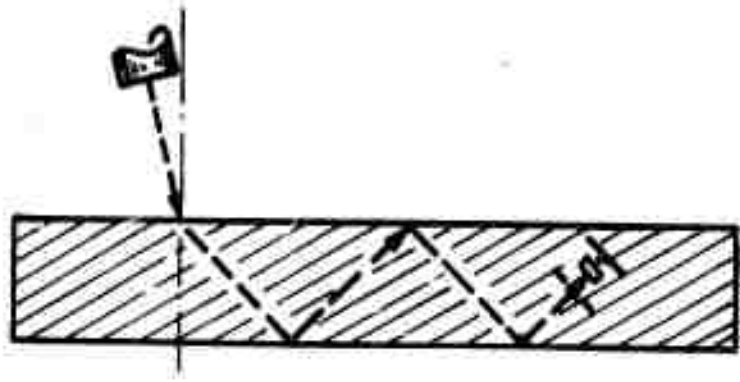
FIGURE 5   MULTIPLE REFLECTION TRANSDUCER GEOMETRY
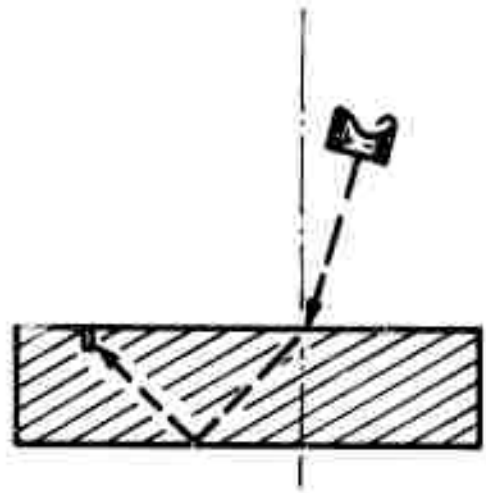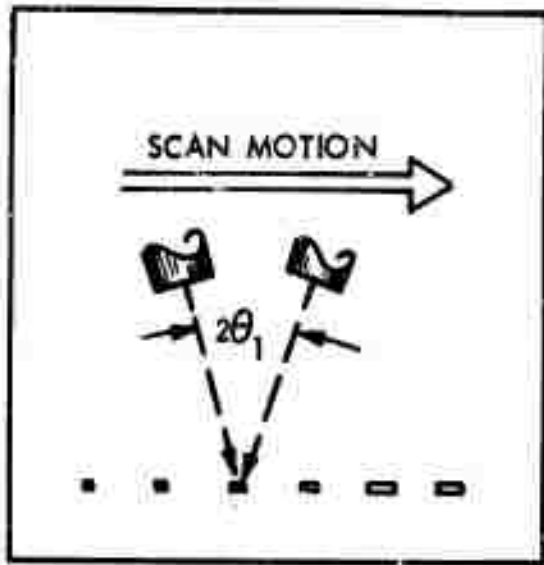
DIFFERENT VALUES OF θ PRODUCE
DIFFERENT BACKGROUND NOISE
PATTERNS BUT SIMILAR FLAW
INDICATIONS
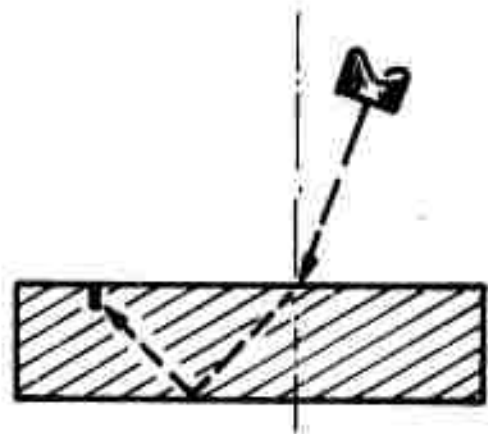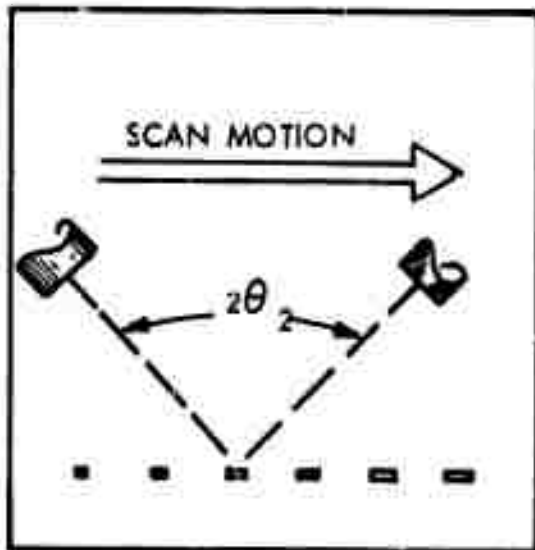
FIGURE 6   DUAL TRANSDUCER CONFIGURATION

9

PLANE #2

PLANE #1

SIDE VIEW

END VIEW

WELD

PLANE #1

PLANE #2
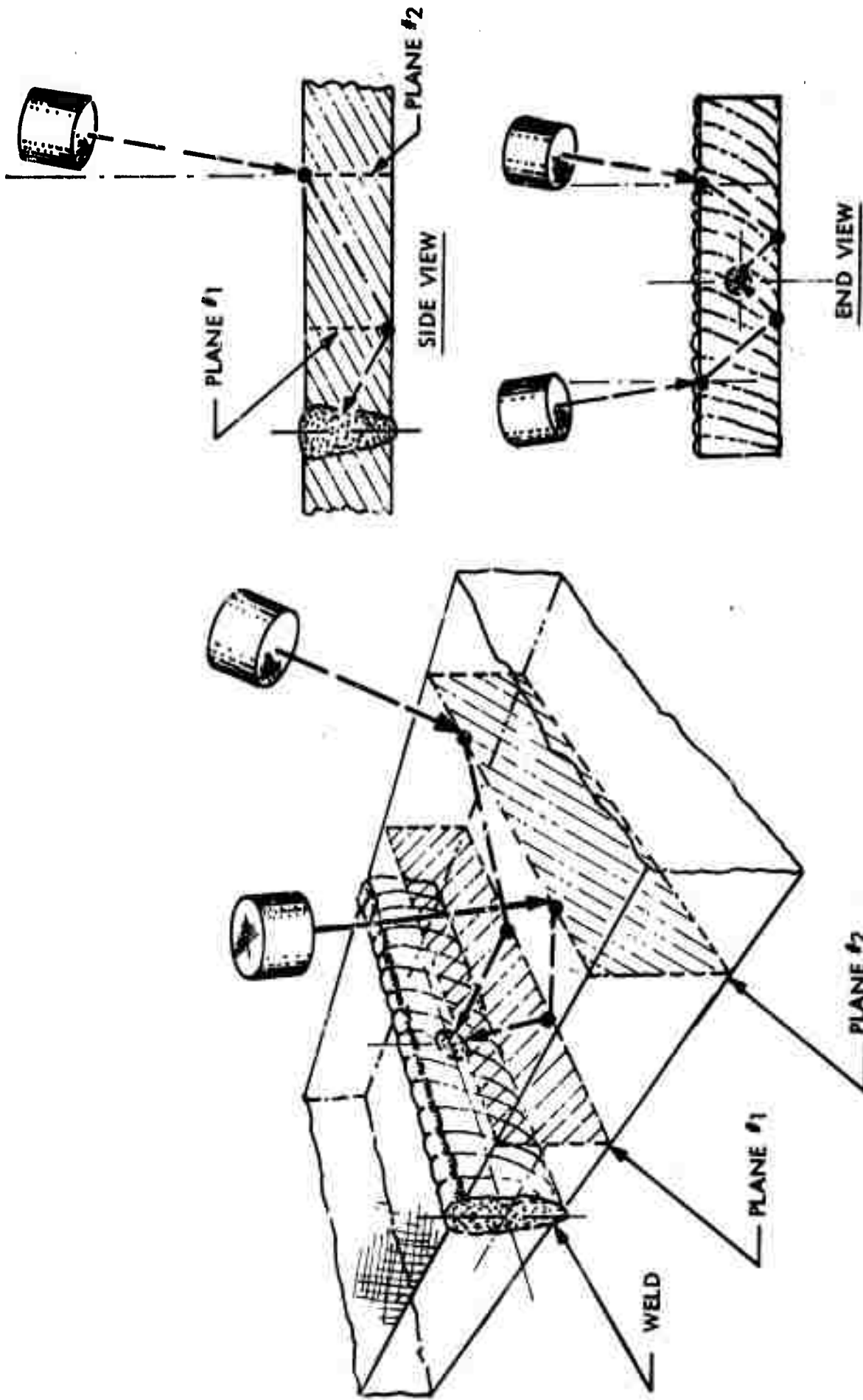
FIGURE 7   DUAL TRANSDUCER CONFIGURATION
IN PERSPECTIVE

10

FIGURE 8 DUAL TRANSDUCER CONFIGURATION WITH 20° INCLUDED ANGLE

A tape recorder was used to produce the product data. The data seen in Figures 11, 12, and 13 were recorded on separate FM channels of an Ampex SP300 tape recorder, and were passed through an analog multiplier upon playback. The tape recorder and multiplier can be seen in Figure 9. Figure 10 is a block diagram of the electronics. The multiplier is an Analog Devices 426A Multiplier/Divider. It is a small, relatively inexpensive, solid state device. Seen also in Figure 9 are the multiplier power supply and the brea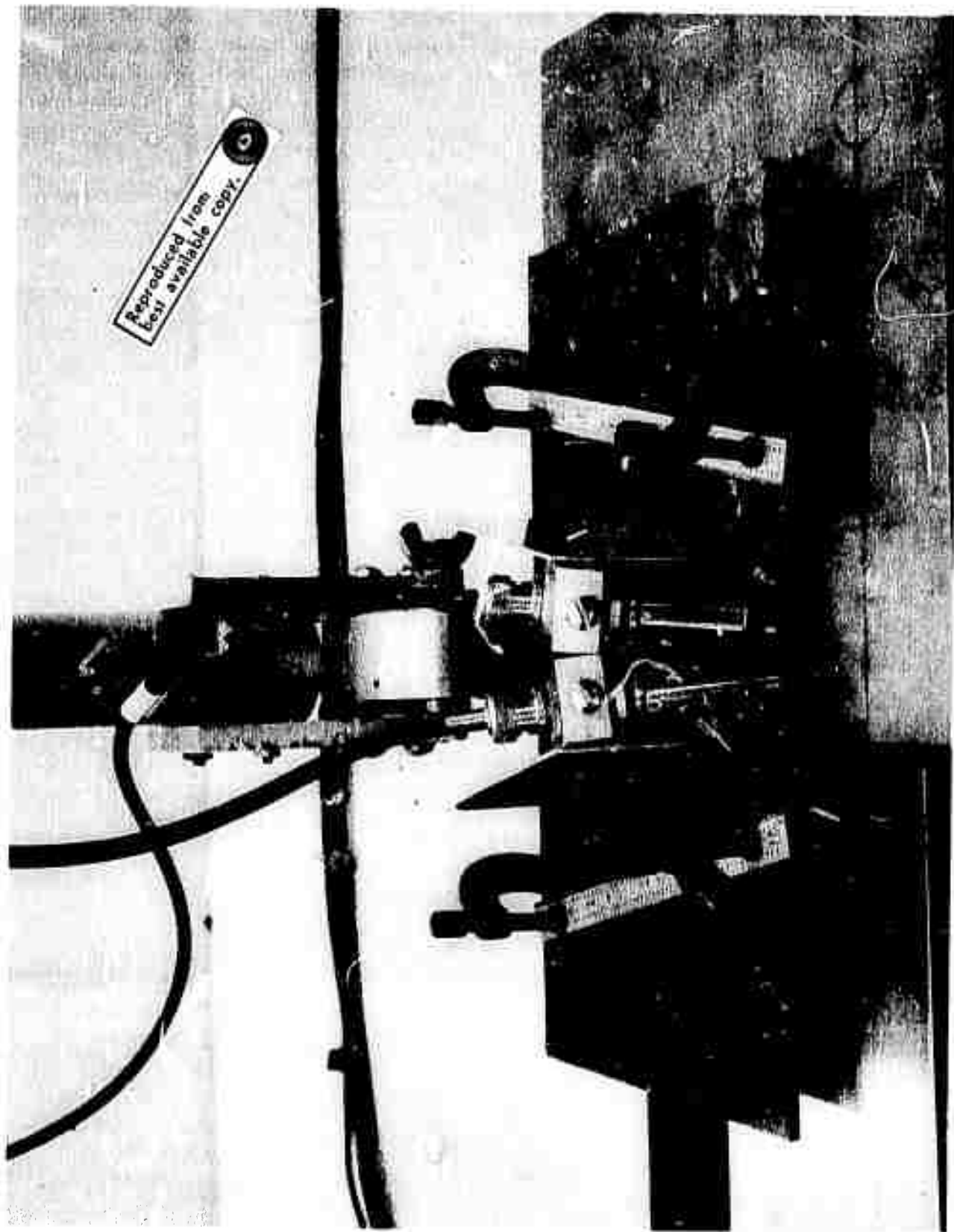dboard DC amplifiers and level shifters which form the interface between the tape recorder and the multiplier. Using two multipliers the triple product could be formed readily with one playback operation. To produce the data reported here, however, the zero degree and forty degree data were multiplied together and the result was recorded on tape. A pen recording of the first product can be seen in Figure 14. A second playback step was used to multiply the first product by the sixty degree data. A pen recording of the triple product can be seen in Figure 15.

Proper alignment of the data on the various channels of the tape recorder is essential. If the data is not accurately aligned, flaw indications can be lost by taking the product. Several conditions are required to obtain properly aligned data. The SP300 record mode must be automatically initiated when the scanner reaches a given position along the length of the weld. The position in question can be defined by the receipt of an echo from a hole in a beam position indicator lined up with the weld. A microswitch and relay can be used to start the recorder. In addition, the magnetic tape must start from the same place each time. Immediately preceeding initiation of the record mode for a given scan along the weld, the magnetic tape must be placed in a given position, accurate to several millimeters, relative to the record head. Finally, since the recorder tape drive operates at a constant speed the scanner must move at a constant speed. If this condition is not met the data may be aligned at the beginning of a given scan but not at the end. Use of an AC synchronous motor to drive the scanner was adequate for the present work.

Data and Conclusions

The data shown in Figure 11 was taken from that portion of the test specimen containing the six artificial flaws, (Figure 1). Four of the "flaw" indications are readily distinguishable, one is marginal and the last is not distinguishable from the surrounding noise background. The large peak on the left is due to an edge reflection. The majority of the background noise appears to be due to the surface roughness of the plate and to the granularity of the titanium metal. Knowing the location of the artificial flaws enables one to locate the probable flaw indications even for the two marginal signals in the present data. The locations are indicated in Figure 11. Note that the curve contains a number of other peaks of height and shape approximately the same as that of the smaller of the two ten mil drill hole indications. The approximate signal to noise ratio for the smaller ten mil drill hole indication is one to one.
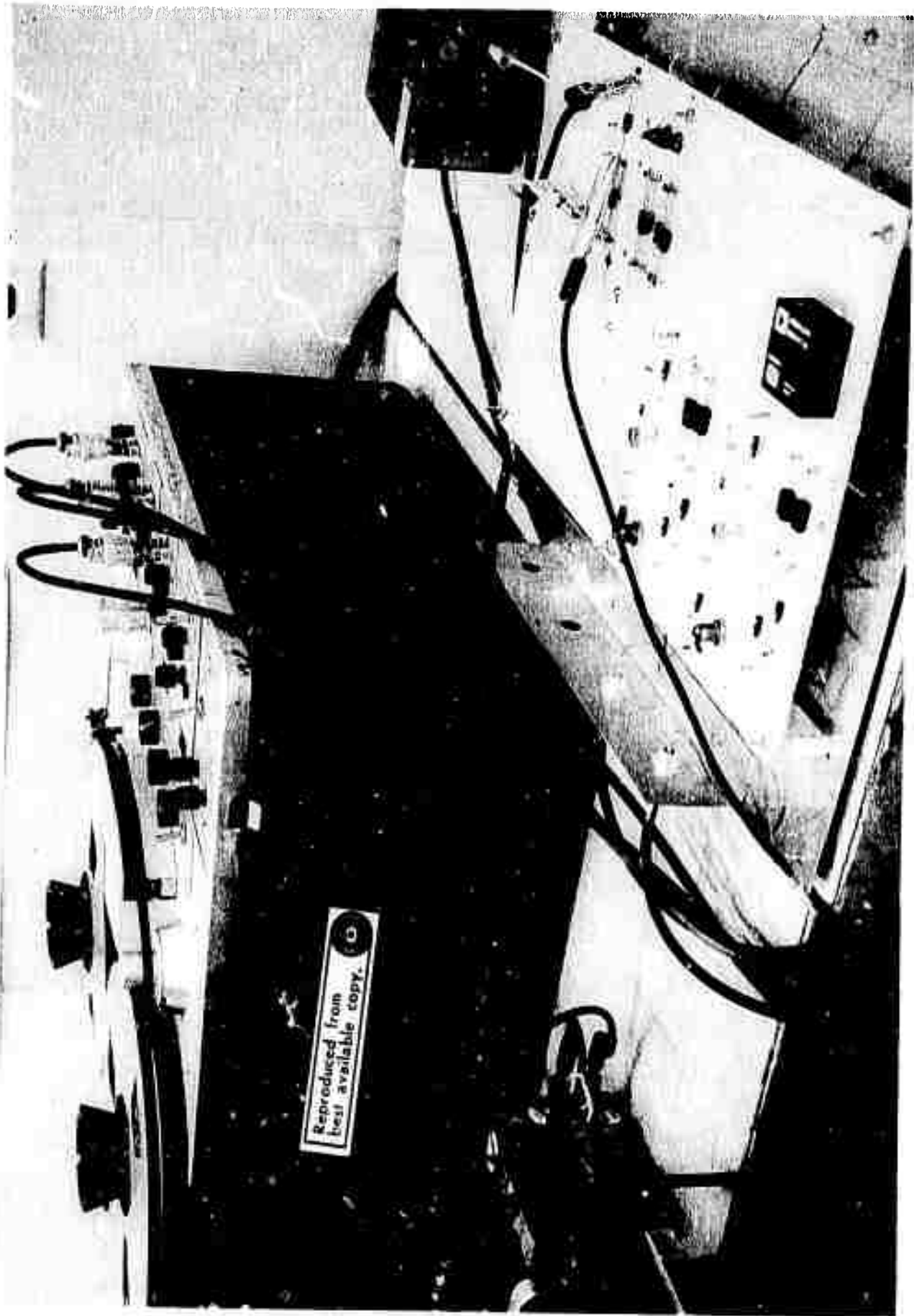
FIGURE 9 TAPE RECORDER AND MULTIPLIER
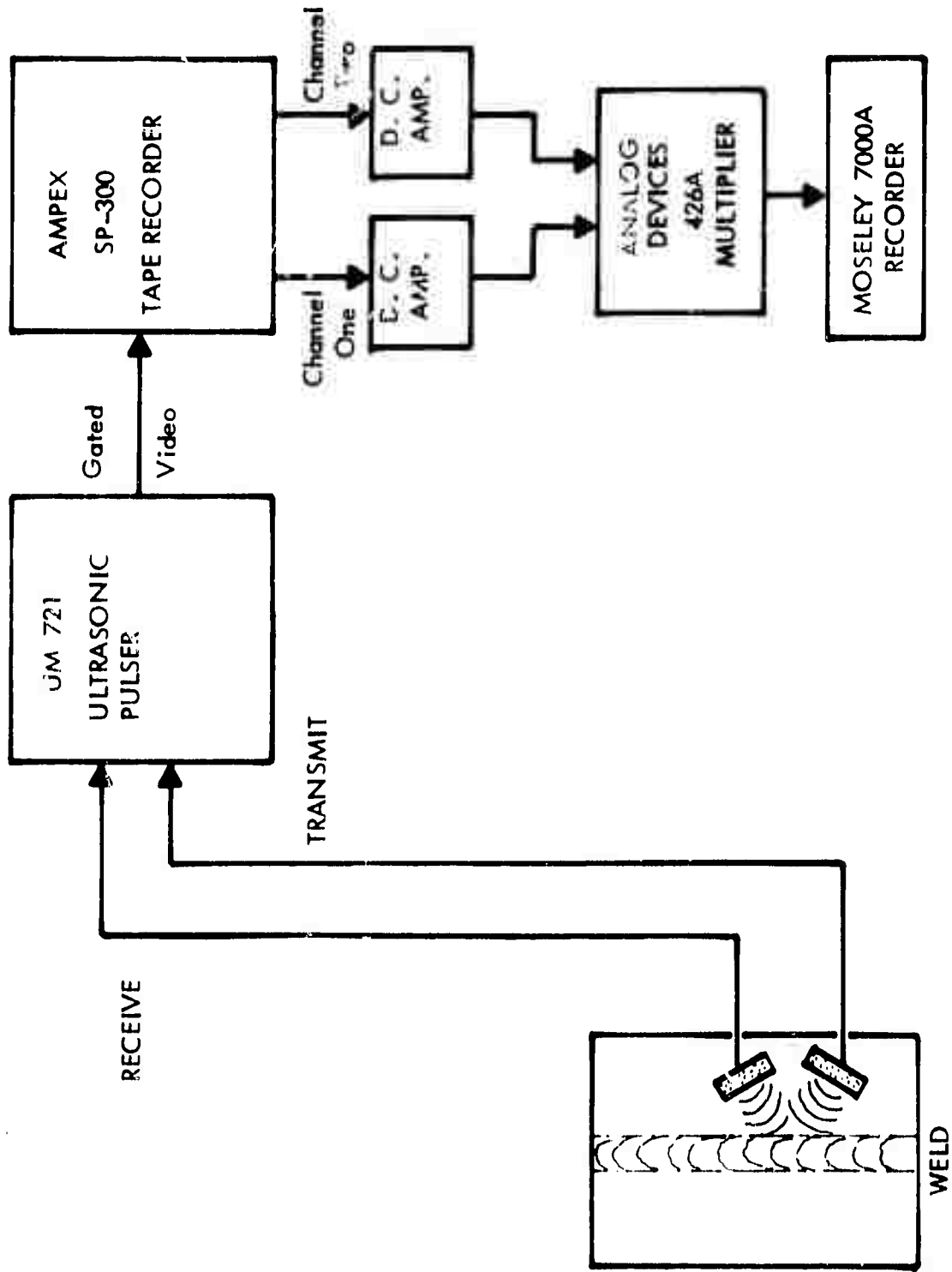
13

FIGURE 10   BLOCK DIAGRAM OF EQUIPMENT USED FOR TAPE RECORDING AND
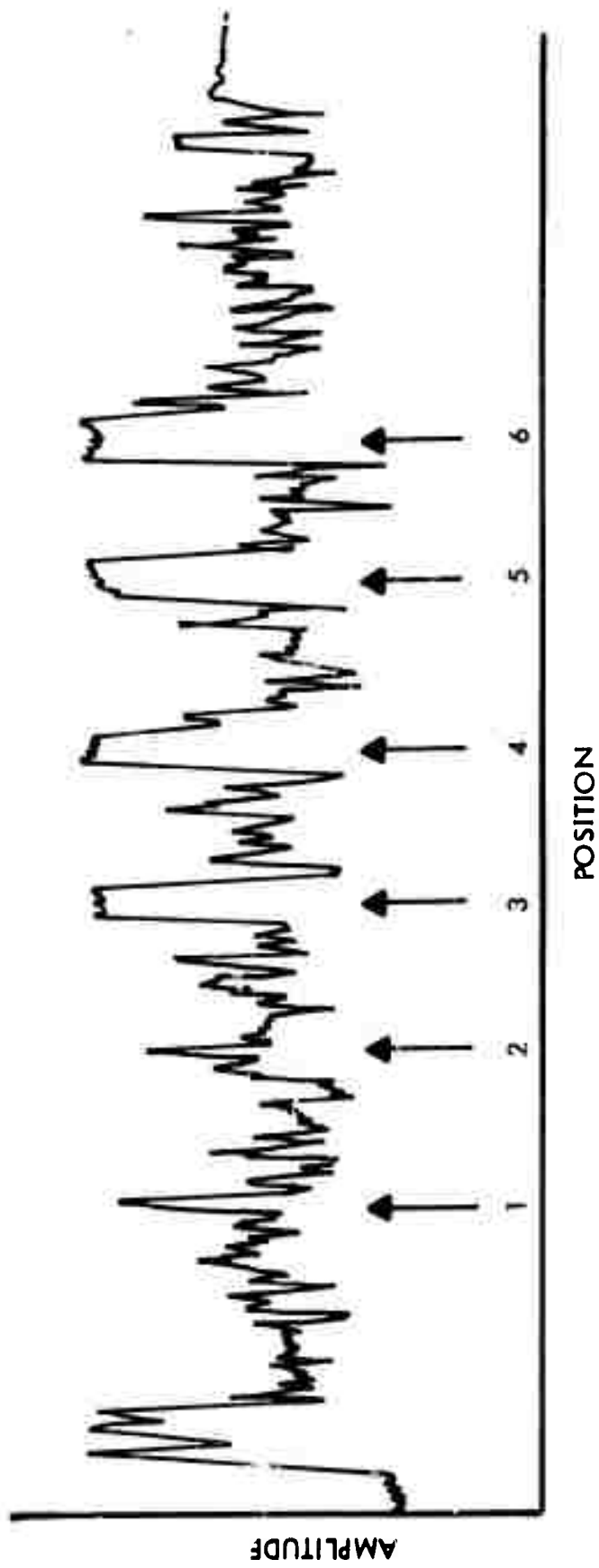MULTIPLYING ULTRASONIC WELD INSPECTION DATA.

14

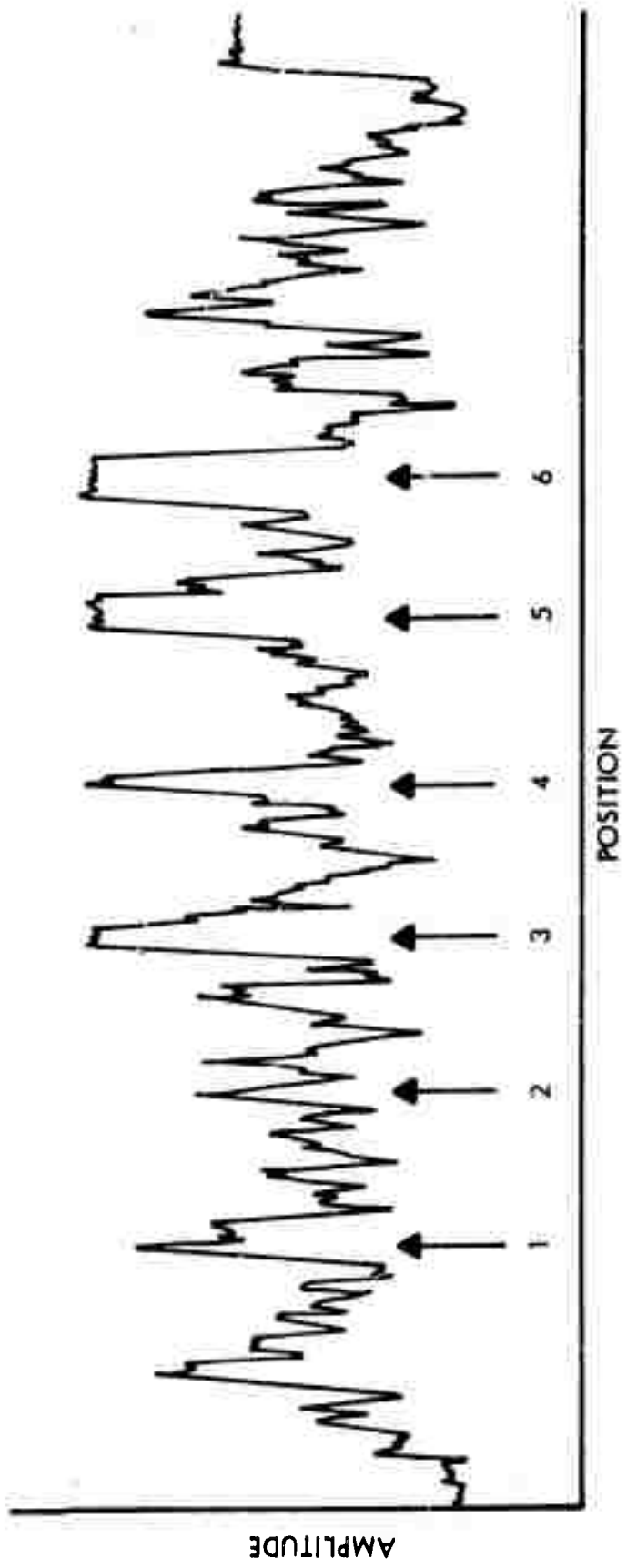FIGURE 11   CONVENTIONAL OR ZERO DEGREE DATA

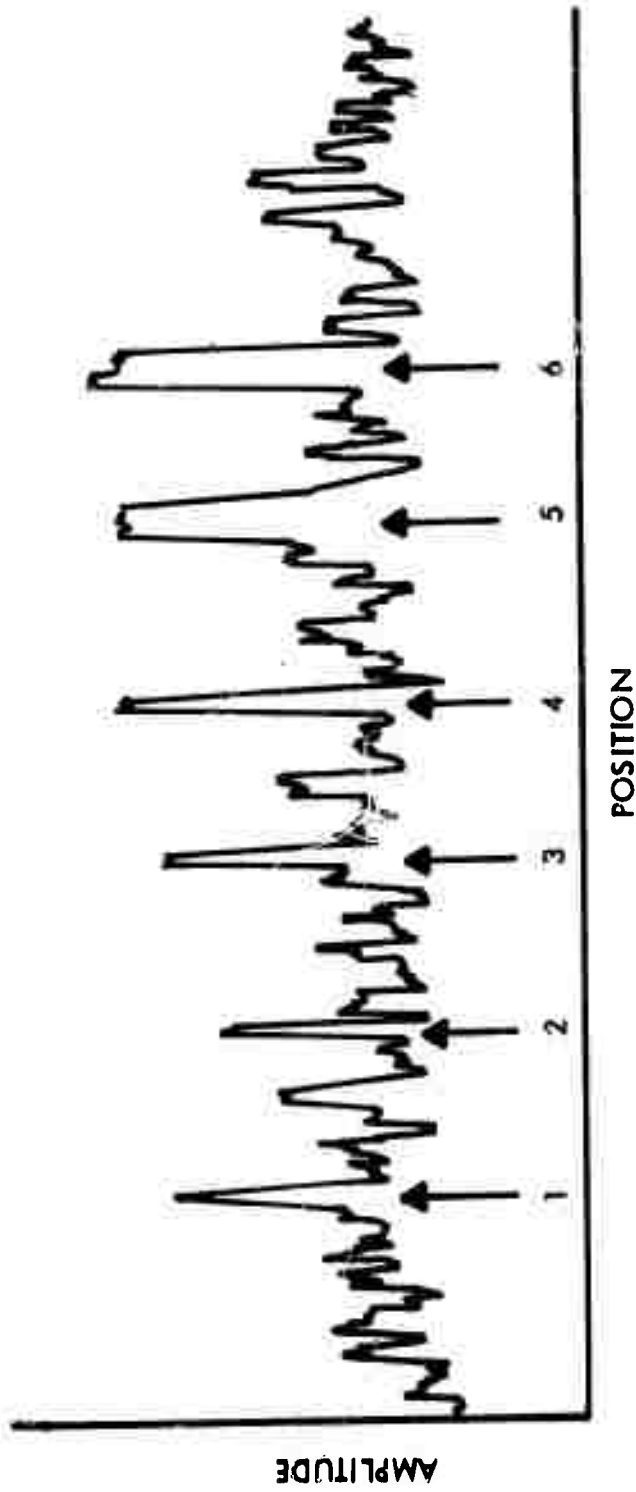FIGURE 12   DATA FOR 40° INCLUDED ANGLE DUAL TRANSDUCER CONFIGURATION

FIGURE 13   DATA FOR 60° INCLUDED ANGLE DUAL TRANSDUCER CONFIGURATION

17

The data shown in Figures 12 and 13 were also taken from the region of the test specimen containing the artificial flaws. Note that the signal to noise ratio is approximately the same for all three sets of data; the zero degree or conventional data, the forty degree data, and the sixty degree data. The approximately equal quality of the data is important because improvement is unlikely if the product is taken between good and bad sets of data. Note also that each set of data exhibits a different background noise pattern. This is essential if the multiplication process is to reduce the general level of background noise. It is believed that the background noise patterns are different because, in each case, the sound enters the part at a different location and subsequently follows a different path.

Figure 14 shows the product of the zero degree and forty degree data. Note that a significant number of extraneous peaks have been removed. The signal to noise ratio appears to be on the order of two to one or two point five to one. Figure 15 shows the triple product. In this curve the signal to noise ratio has increased to a value of about five to one. Some peaks of unknown origin at the right end of the scan continue to be retained.

Although correlation produces impressive improvements in signal to noise ratio, it is unlikely that the procedure we have described will reliably yield satisfactory raw data. This is due to the fact that ultrasonic signals are typically sensitively dependent upon transducer position and orientation. A small change in transducer position can produce a large change in the ultrasonic signal obtained from a localized scattering center. Consequently, small errors in transducer position during initial setup can produce large changes in the signal to noise ratio of the flaw indication. If the signal to noise ratio of the flaw indication in any of the factor curves is less than 1 to 2 the multiplication process may not improve matters and if it is greater than 3 to 1 multiplication is not needed.

If however one sets up an array of transducers in the configuration of Figure 17, one can take advantage of the position sensitivity and still find opportunities to improve marginal signals by correlation. Under these conditions a number of signals are available for correlation and signal to noise improvements can be obtained by forming properly chosen products. If a flaw signal appears clearly in any of the original data curves there will, of course, be no need for correlation to establish its presence. If marginal signals occur at approximately the same place in several of the curves a product of those curves may make a significant improvement in the clarity of the signal. The process could be made automatic by feeding all possible products into threshold level alarm systems. Details of the work performed on real time correlation with a multitransducer array appear in the next section.

MULTIPLICATION OF ULTRASONIC DATA IN REAL TIME

Specimen

The specimen used for this portion of the work is shown in Figure 16. The plate is of 6Al-4V titanium metal and contains ten end cut drill holes as shown in the diagram.
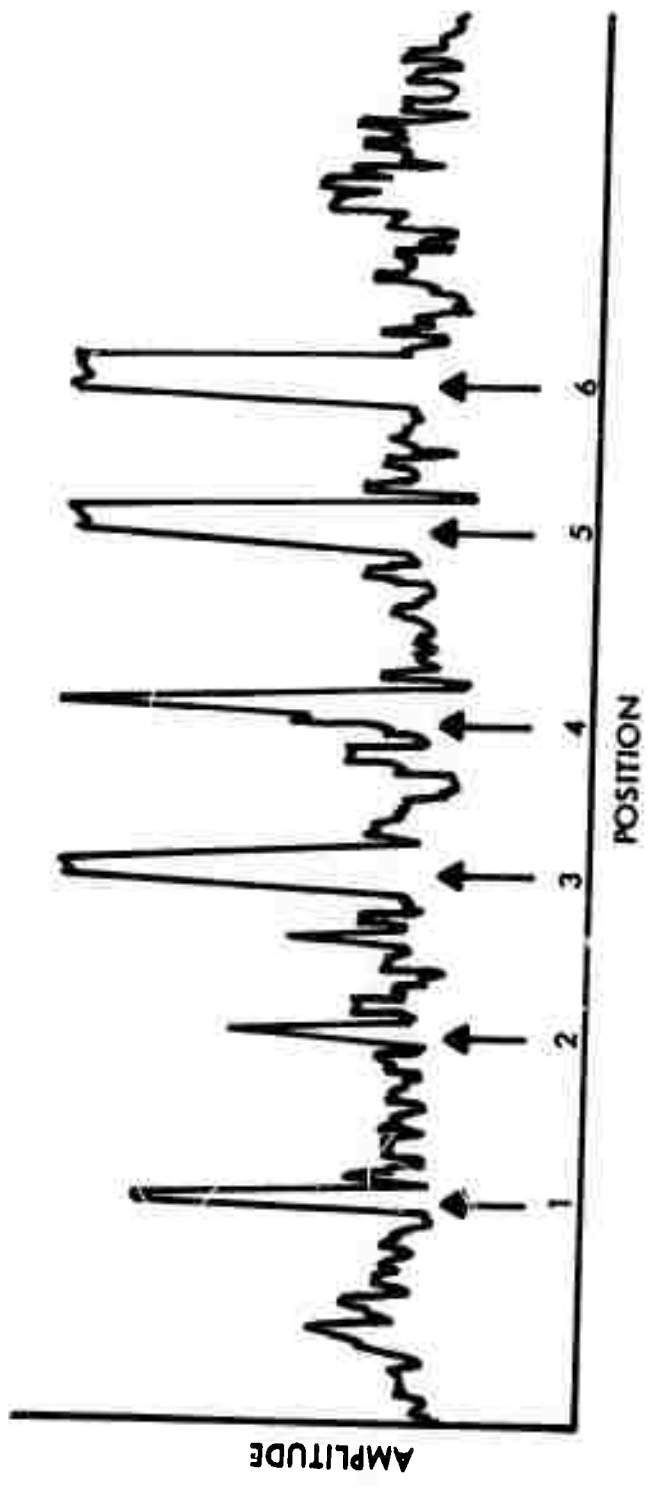
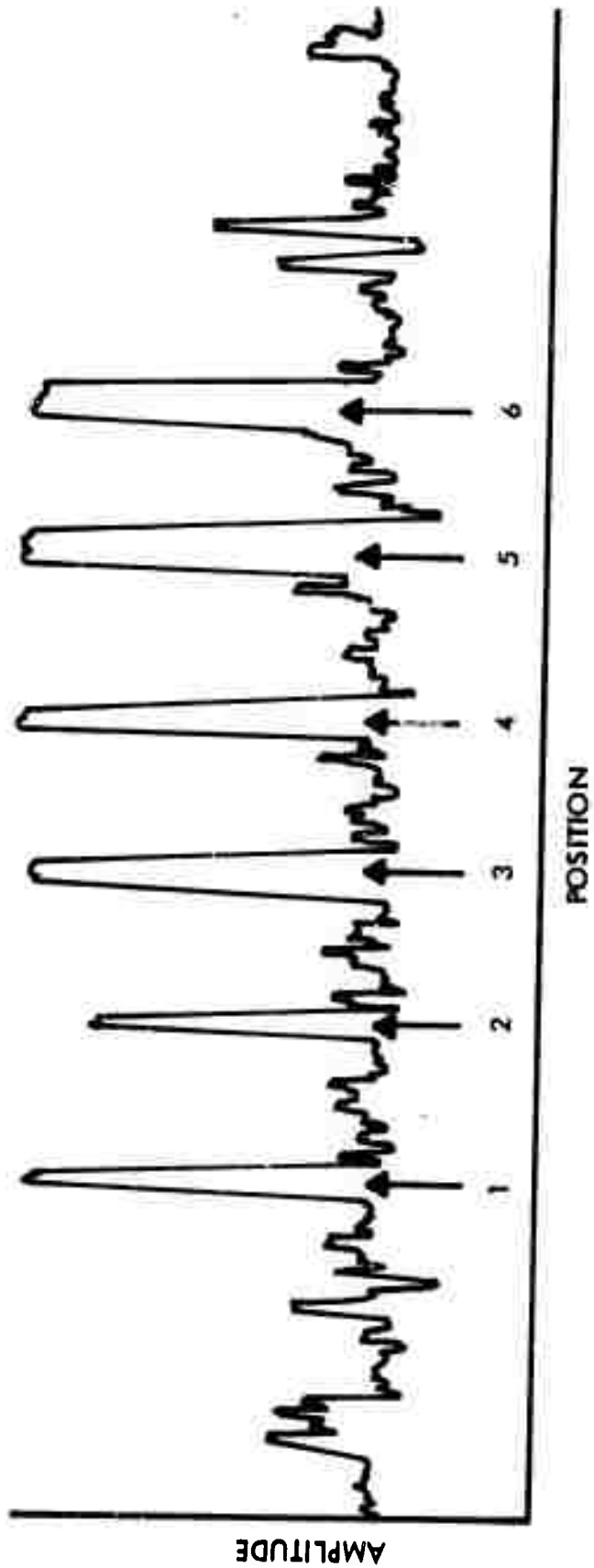FIGURE 14   PRODUCT OF 0° DATA AND 40° DATA

19

FIGURE 15   PRODUCT OF 0°, 40° AND 60° DATA

20

These holes, five flat bottom and five round bottom, are intended to be representative of totally interior cracks. As before, the specimen was examined as if it contained a weld seam with possible flaws. As shown in the diagram the centerline of the "weld" was taken to be a line 1/2 inch in from the edge.

Equipment and Procedure

The specimen of Figure 16 was inspected using the five transducer array shown in Figure 17. A schematic representation of the transducer configuration appears as a portion of Figure 18. The array can be considered as an extension to more than two transducers of the arrangement shown in Figure 6 of the previous section. Each of the transducers has the same value of ϕ. The value of ϕ which produced the largest response to the easily visible drill holes was selected.

As can be seen from the diagrams the transducers have various values of θ. The transducers are all directed towards the same weld volume. There are a large number of possible entrance and exit paths providing the opportunity to inspect the weld volume from a number of different aspects without physical motion. Since ultrasonic flaw indications are strongly sensitive to the detailed orientation and geometry of the flaw, an arrangement of this kind is likely to increase the possibility of detecting small localized scattering centers. With adequate electronics a number of signals can be made available simultaneously and correlation in real time becomes a relatively simple matter.

In the present work only one transducer at a time was allowed to transmit, the other four being considered as receivers. In this operating mode the configuration is like a Delta Scan system with a number of receivers. The use of more than one transmitter produces crosstalk the effect of which will have to be the subject of further work. The various one-transmitter combinations were examined using the specimen in Figure 16. As before, recordings were made on an XY plotter. The three transmit receive patterns which exhibited the flaws most clearly were selected. The three signals selected, as shown in Figure 18, correspond to transducer number 3 transmitting and transducers 1, 4, and 5 receiving. It is important to note that none of the signals selected is in an expected specular direction. The data can be seen in Figure 22.

The weld scanning pattern is necessarily different for the multi-transducer array than it is for a single transducer arrangement. The gate location and transducer scanning motion for a conventional single transducer inspection are shown in Figure 19. The transducer shuttles back and forth in a horizontal plane as the weld is inspected from top to bottom. A wide gate is employed which encompasses the weld volume for all positions of the transducer. A motion of this kind is not acceptable for the multi-transducer array because the common point of intersection of the transducers moves in and out of the weld plane as the set of transducers shuttles back and forth. However, if the set of transducers shuttles in a vertical plane the common point of intersection moves up and down in the weld plane and the weld is interrogated in the usual

21

TOP VIEW

10-1/2"

Scan Motion

9-1/2"

1/2"

125 100 50 25 10 125 100 50 25 10
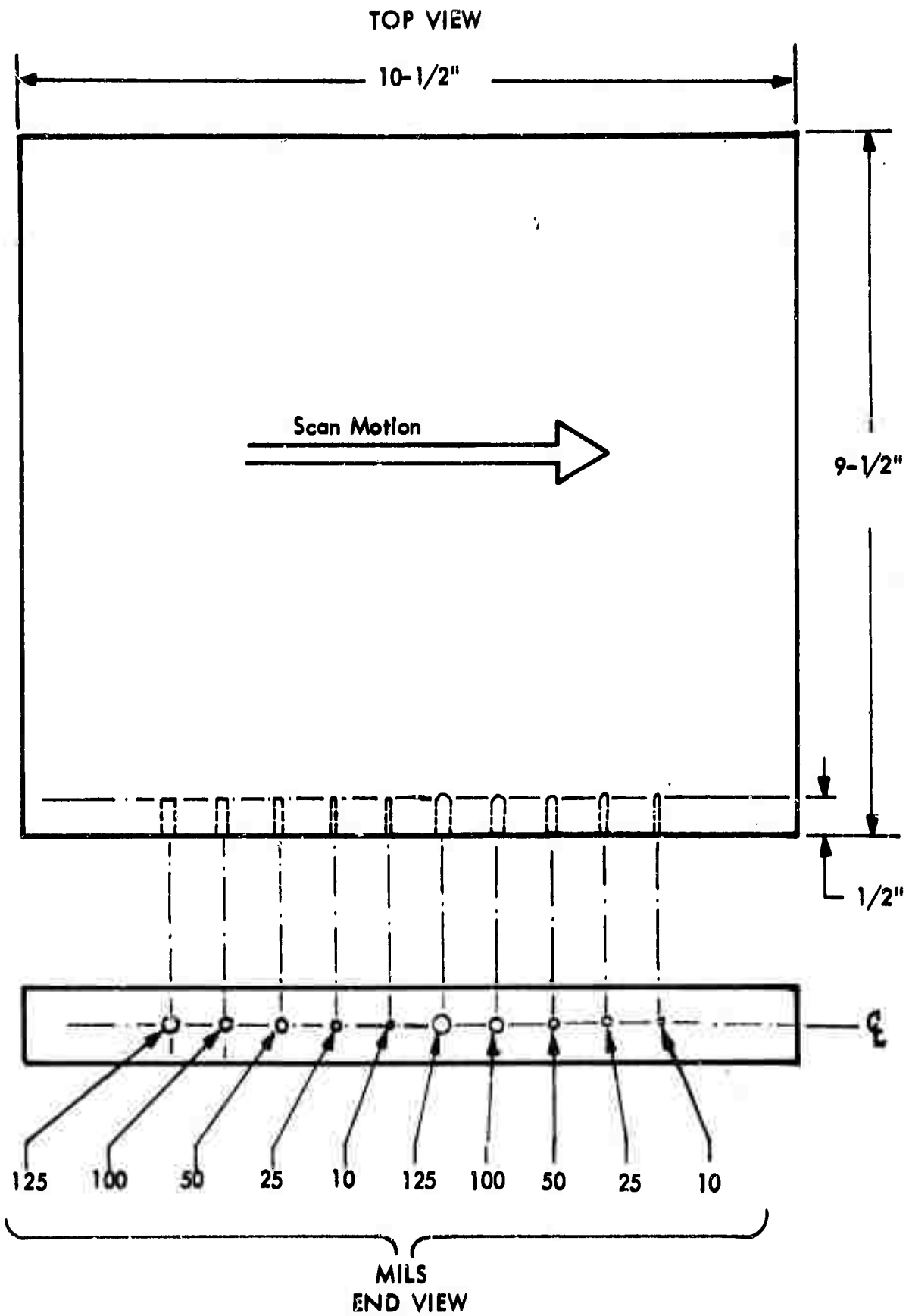
MILS
END VIEW
FIGURE 16   TEST SPECIMEN

22

FIGURE 17 PHOTOGRAPH OF TRANSDUCER CONFIGURATION FOR REAL TIME MULTIPLICATION
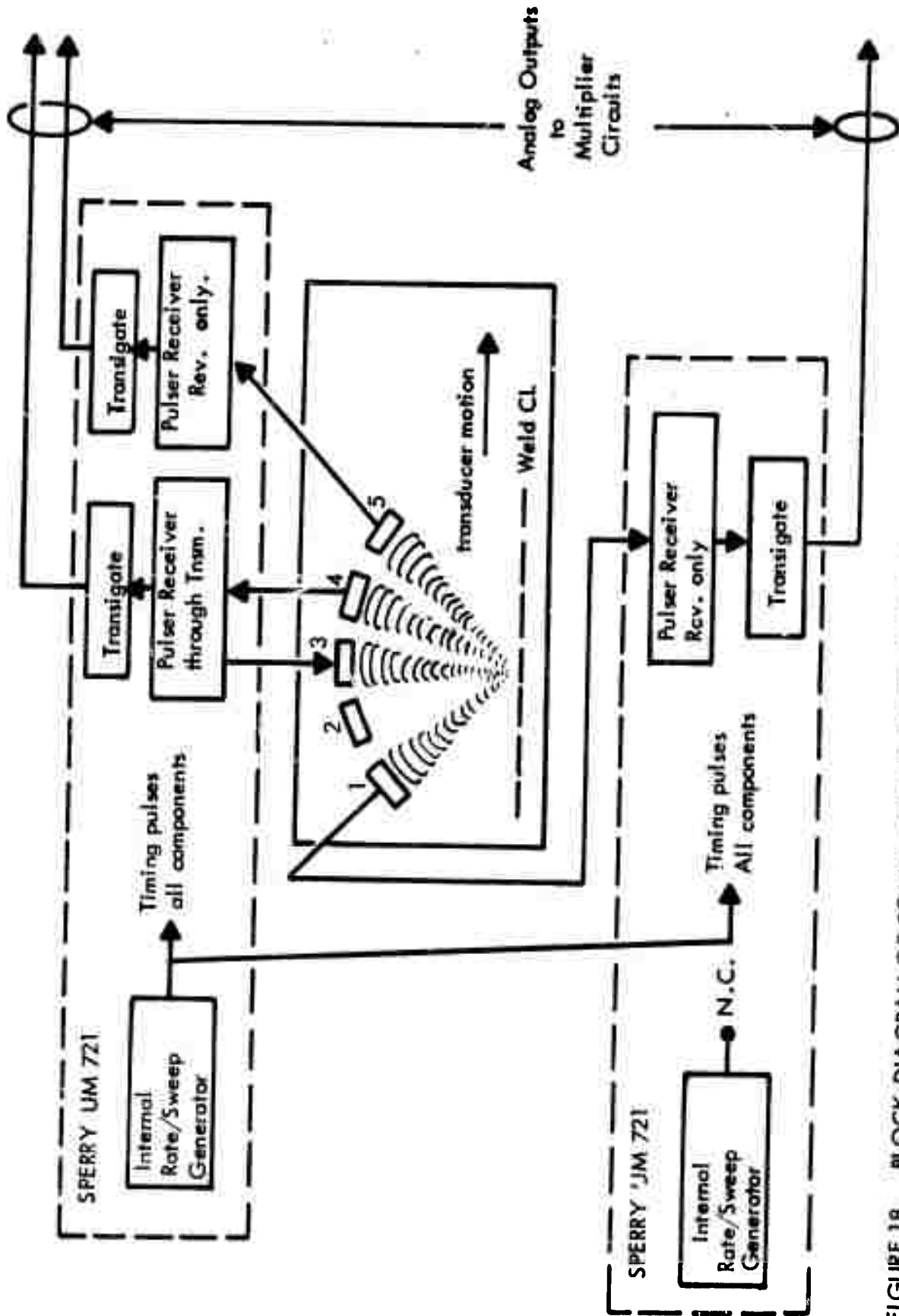
FIGURE 18   BLOCK DIAGRAM OF EQUIPMENT USED FOR REAL TIME
MULTIPLICATION OF ULTRASONIC WELD INSPECTION DATA

24
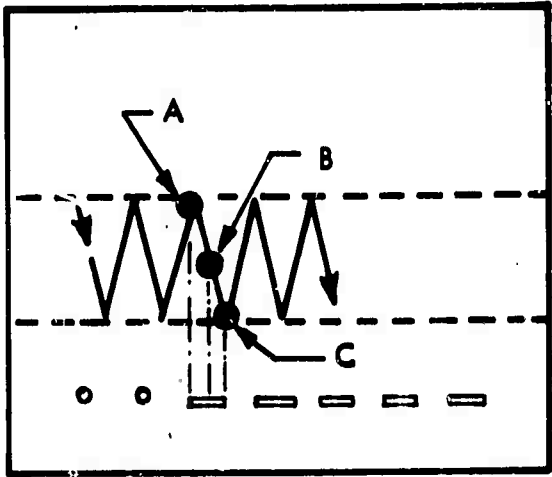
TRANSDUCER MOTION

A, B, and C Show Successive Transducer Positions

Gate Interval

A

Gate Interval

B

Gate Interval

C
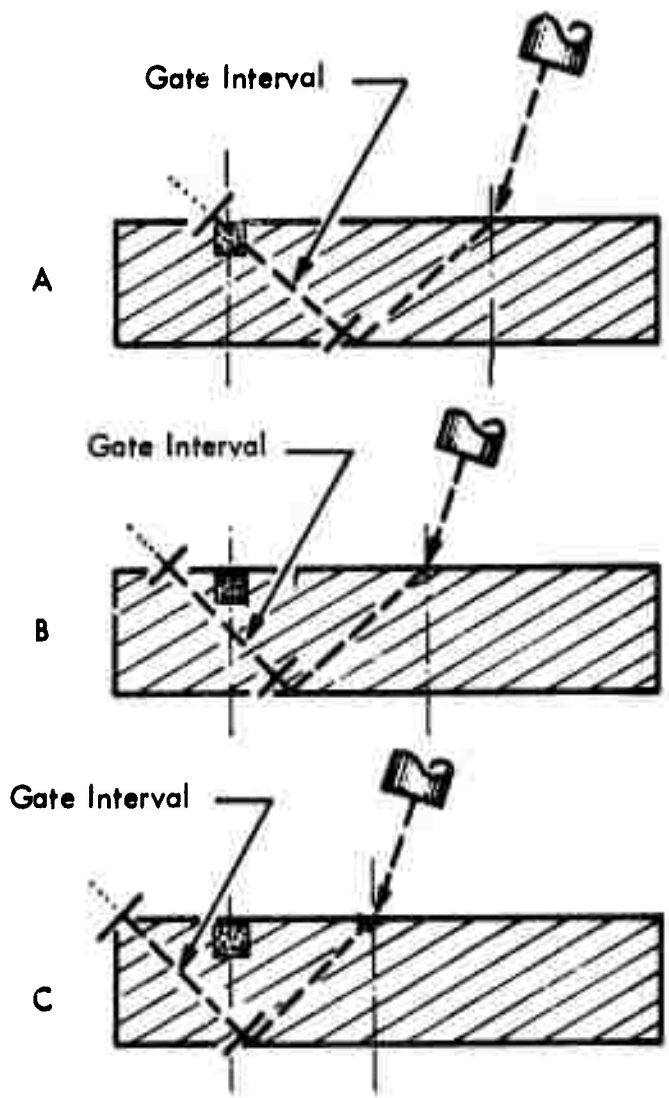
FIGURE 19   CONVENTIONAL WELD SCAN

25

Gate Interval

A

A, B, and C
Show
Successive
Transducer
Positions

B

Gate Interval

Gate Interval

C

FIGURE 20   MULTIPLE TRANSDUCER WELD SCAN

fashion. The motion is depicted in Figure 20. The use of a narrow gate with a variable time delay is also indicated in Figure 20. If a narrow gate is used the gate time delay is a linear function of the vertical position of the set of transducers. Vertical position information can be supplied by a potentiometer attached to the scanner. Electronic circuitry for a variable time delay gate is available. We have previously discussed the operation of such a gate from a position indicating potentiometer[2]. Use of a narrow gate rather than a wide gate considerably reduces background noise.

The transducers used for the real time multiplication work are all 1/2 inch diameter 5 MHz crystals. The five transducers, purchased as a group so that their properties would be similar, were obtained from The Zetec Corporation. The transducer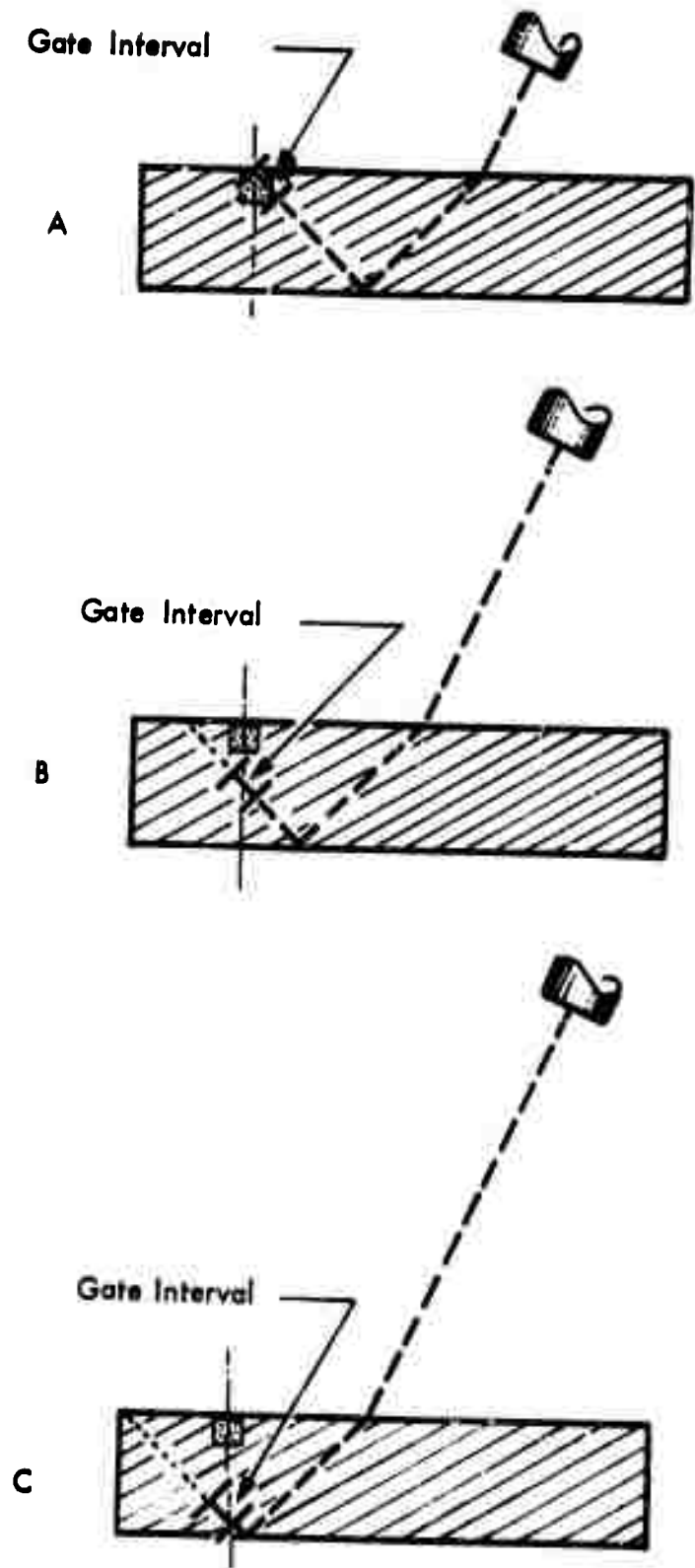s need not be identical, but if they are similar system operation is simplified. The system electronics can be seen in the block diagram of Figure 18. Two Sperry UM721 Reflectoscopes are synchronized together. One Reflectoscope is operated with two pulser-receiver units and the other is operated with one pulser-receiver unit. This arrangement provides enough amplifiers and gates to handle three signals at the same time. The signals are amplified, detected, and gated in the Sperry circuitry, and the transigate outputs are connected to the multiplier circuitry shown in Figure 21. The amplifiers shown in Figure 21 perform the amplification, inversion, and level shift necessary to fit the dynamic range of the transigate output into the ten volt range required by the multipliers. They are adjusted so that the linear portion of the transigate output is fit into the range 0 to 10 volts positive. The triple product is produced by two Analog Devices 426A multiplier units connected as shown in the diagram.

Data and Conclusions

The three recordings which most clearly exhibit the ten artificial flaws are shown in Figure 22. Individual drill holes can be identified by comparing Figure 22 to Figure 16. The flat holes are on the left and the round holes are on the right. There were other recordings, some of which contained inferior indications of the 10 and 25 mil drill holes. Those recordings were intentionally excluded from the product because it was known that no improvement would result. Decisions of this kind are possible in real inspection situations if one is performing a lengthy and detailed examination of a weld sample. In an inspection line situation all possible products would have to be automatically calculated and fed into threshold level alarm systems. Since a large number of signals are possible a small on-line computer is indicated for this operation. The multiplication and alarm triggering could be done in digital form.

No one recording shows all of the flaws cleanly, but each of the recordings contains some indication of all ten flaws. Indications from even the smallest flaws appear clearly somewhere in the set of three data curves. This reveals the difficulty we have had producing artificial flaws whose indications have a signal to noise ratio of 1 to 1 or less. Even with the present data however, it is possible to demonstrate considerable signal to noise improvement by correlation.
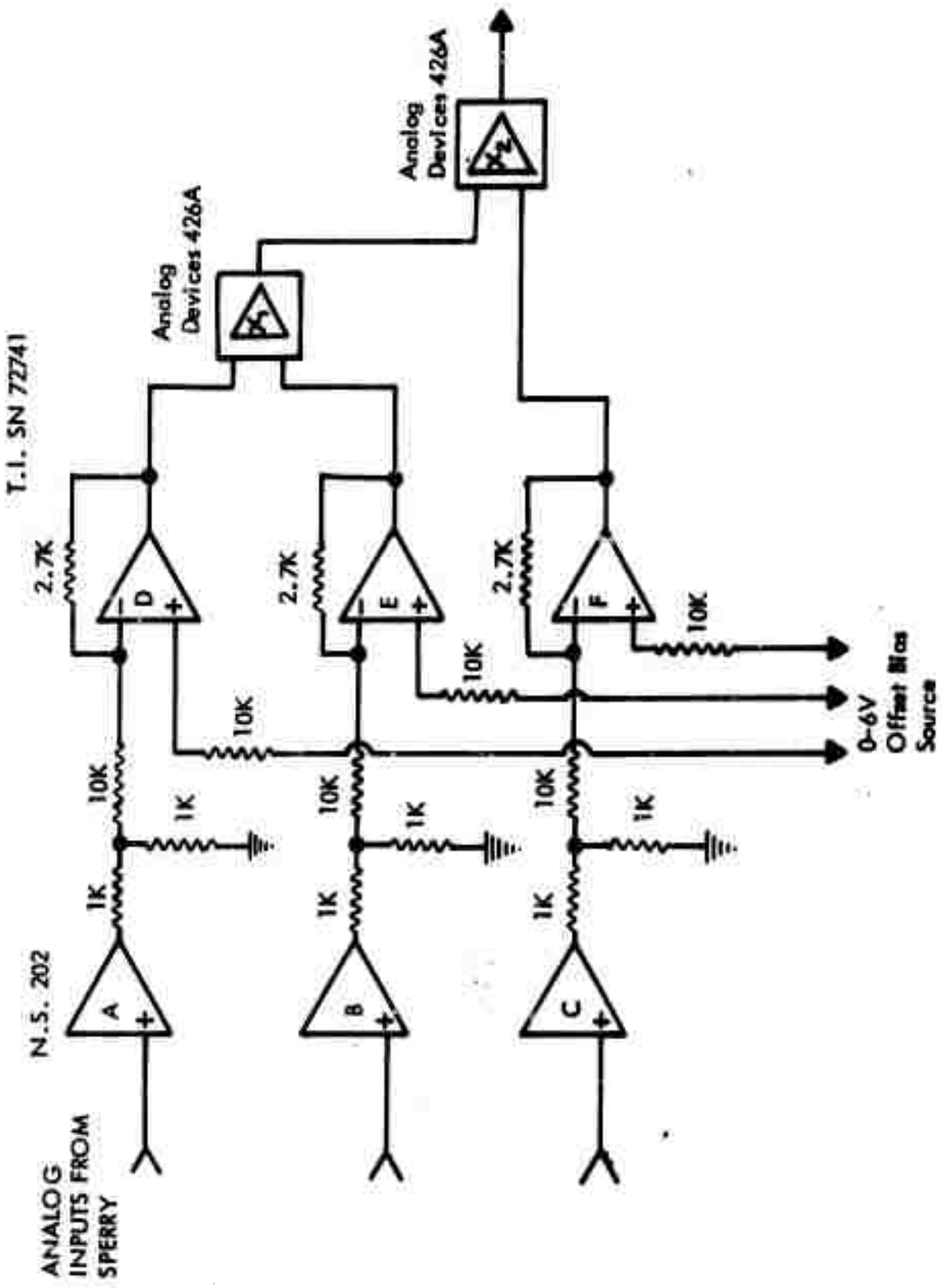
FIGURE 21   MULTIPLIER CIRCUITRY

28
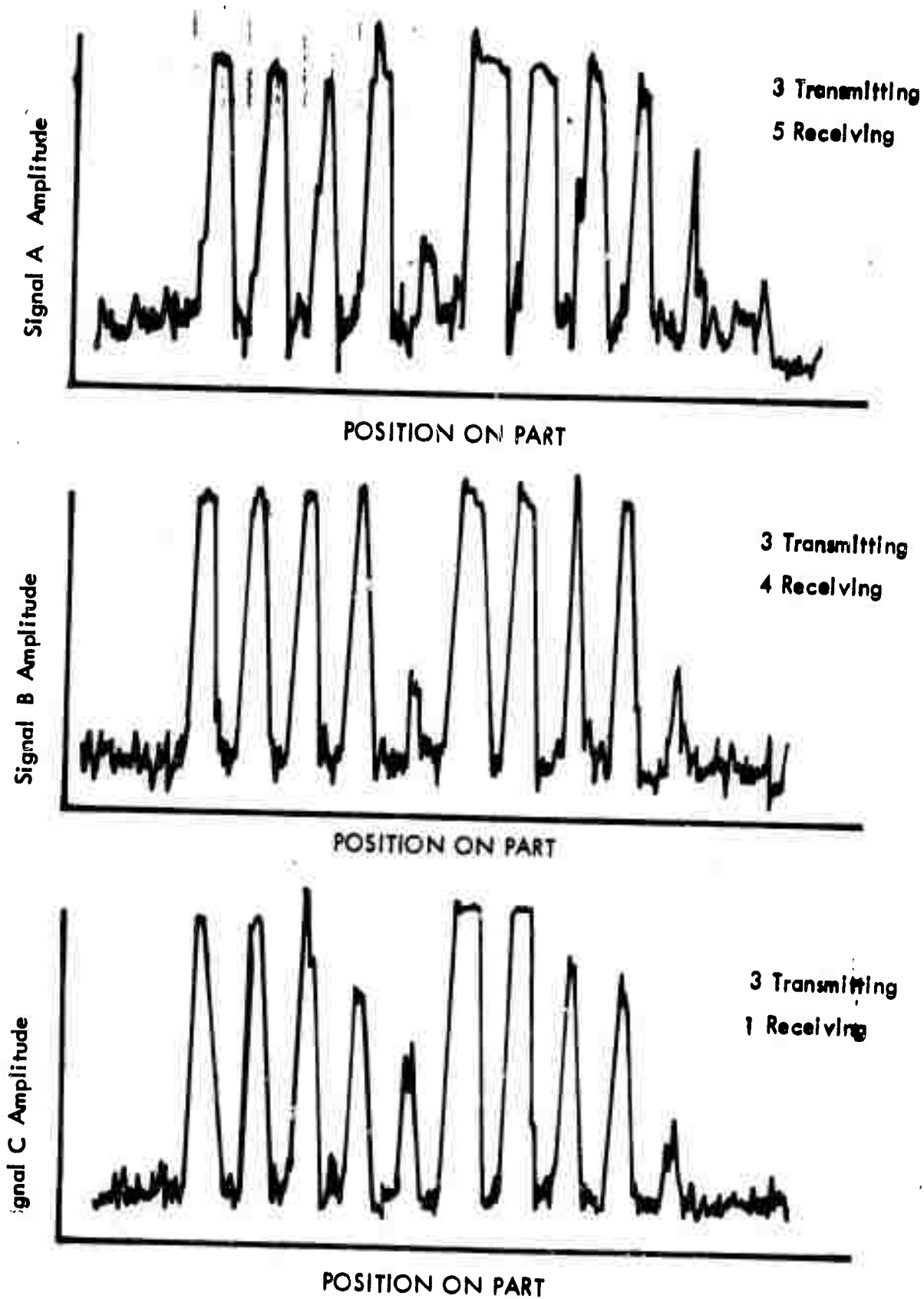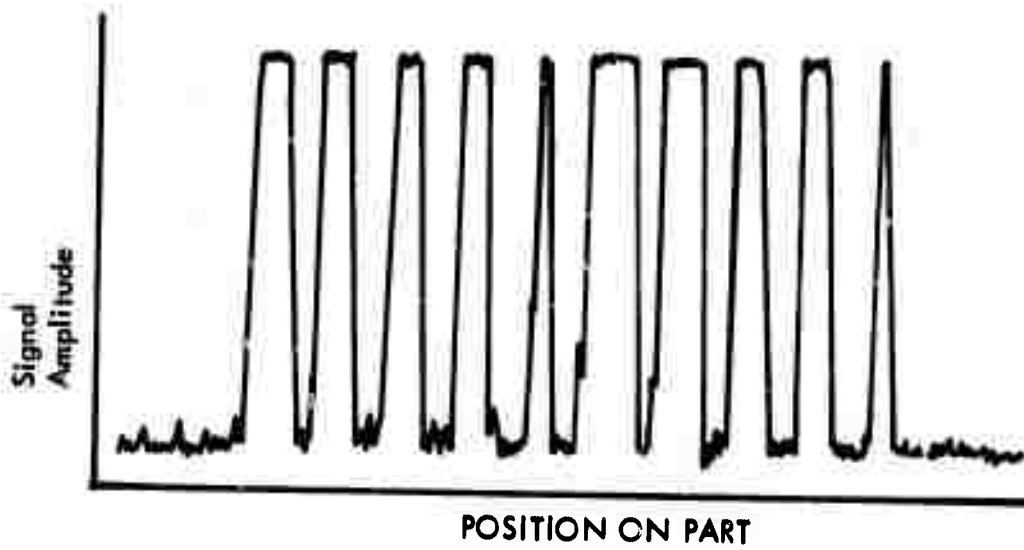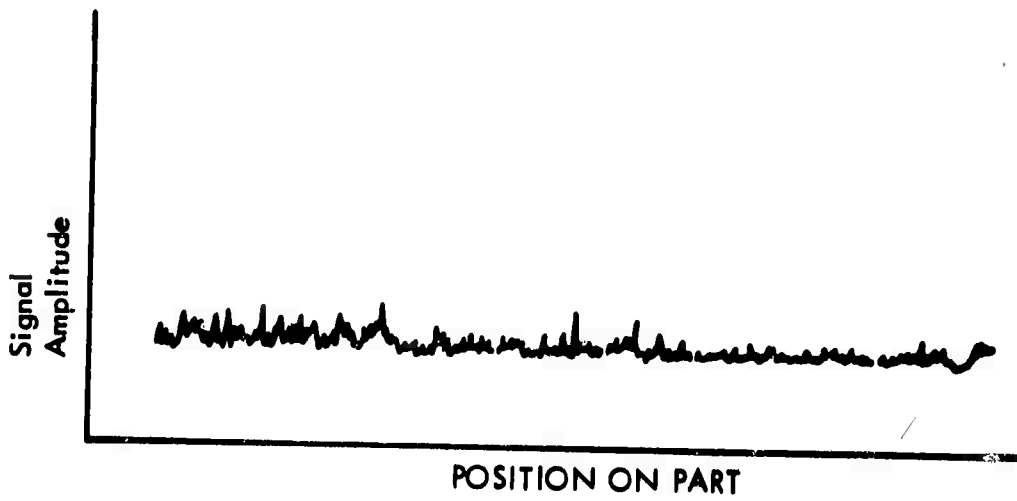
FIGURE 22   ULTRASONIC INSPECTION DATA
PRIOR TO MULTIPLICATION

29

FIGURE 23   REAL TIME PRODUCT OF THREE
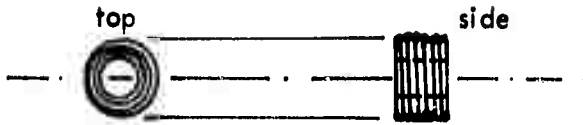SEPARATE ULTRASONIC SIGNALS

The real time triple product curve can be seen in Figure 23. Also shown there is a triple product curve taken from a region of the part known to contain no flaws. All ten flaws are now clearly visible in one recording. Comparison of Figures 22 and 23 reveals a considerable improvement in signal to noise ratio.

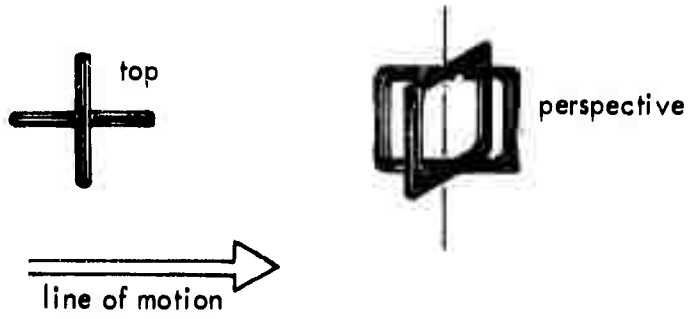## CORRELATION METHODS IN EDDY CURRENT CRACK DETECTION

Theory

Eddy current crack detection systems are commonly limited in sensitivity by background noise due to surface roughness. Even when the surface roughness is acceptable from a metallurgical standpoint, roughness indications can exceed the indications obtained from small cracks. In the present work correlation methods have been used to reduce surface roughness noise. We have used a multiple coil probe which produces four eddy current signals. The four signals contain similar flaw indications but exhibit different background noise patterns. As the eddy current probe scans over the part, a real time quadruple product is formed from the four signals. A considerable improvement in the clarity of the flaw indications results.

Conventional eddy current coils contact the test part in the manner shown in Figure 24a. Background noise due to surface roughness and liftoff can frequently be reduced by using differential coils. The differential coil in a typical commercially available instrument contacts the test part in the manner shown in Figure 24b. The coils are balanced in opposit arms of an AC bridge. A response is obtained only when the part causes the coil impedances to be unequal. Probe liftoff and tilt tend to affect both coils and the instrumentation produces only a moderate response. A sharp crack however is likely to affect one coil more than the other and a clear response is obtained. The probe is normally oriented with respect to the line of motion as shown in the diagram. The coil perpendicular to the line of motion usually produces the sharp crack response, and the coil parallel to the line of motion provides the liftoff compensation. In Figure 24c is shown a differential coil which has the virtue that it can be brought into close proximity with several other coils of the same design. In Figure 24d several such coils have been fitted together into a configuration which can be incorporated into a single probe. Four signals can be obtained from such a probe. Each signal originates in a pair of differential coils. In general, the four signals are different because the coils which provide liftoff compensation contact the part in different places. As a result the eddy current surface roughness noise is different for each signal. However, since the four crack response coils are closely grouped, they all inspect the same portion of the part and they respond simultaneously to any cracks which may be encountered. The eddy current crack response is therefore the same for each signal. The cross-correlation of signals with the above characteristics tends to reduce background noise and enhance flaw indications. Sections to follow will describe the correlation of signals obtained from a probe like the one in Figure 24d. Improvements in the signal to noise ratio of flaw indications will be demonstrated.

top   side   24a

top   perspective   24b

line of motion

perspective   top   24c

B   A   C   D

B   C   A   D   24d

line of motion
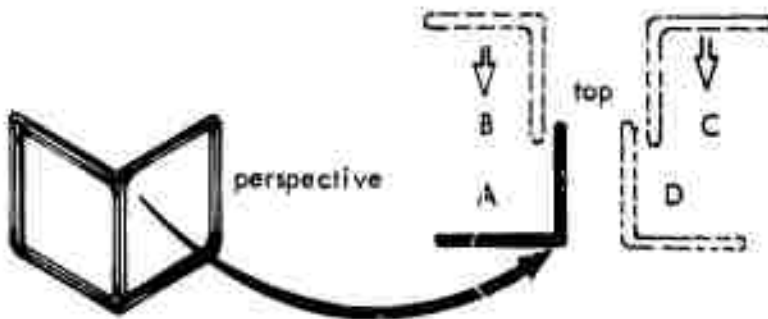
FIGURE 24   EDDY CURRENT TEST COILS

32

MULTIPLICATION OF·EDDY CURRENT DATA IN REAL TIME

Specimens

A diagram of the test part used for the eddy current correlation work appears in
Figure 25. It is an eighth inch thick 18% Ni steel plate, 4 inches wide and
5 inches long. It contains two artificial flaws in the form of EDM slots located
as shown. To produce the data presented in this report the eddy current probe
was caused to move along the path labeled "scan line". The eddy current data
includes indications from the EDM slots and indications from scratches and
irregularities on the surface of the part. Actually the part is relatively smooth.
Its roughness can be determined quantitatively from the surface profile curve
shown in Figure 25. The surface profile data was obtained from a line parallel
to and 1/8 inch away from the scan line. Also shown in Figure 25 is a photo-
graph of the test part surface. Notice that the surface happens to be ground in
at least two different directions. Correlation techniques were effective in re-
ducing the eddy current surface roughness noise encountered during the inspec-
tion of this test part.

The surface profile of a second test part is shown in Figure 26. This part contains
a number of long surface scratches and deep corrosion pits. Some of these can be
seen in the photograph in Figure 26. Correlation techniques were unsuccessful
in reducing the eddy current surface roughness noise obtained from this part. In
order for the correlation methods to work it is necessary that each of the four sen-
sors in the eddy current probe have a different reaction to the surface roughness.
The rather sizeable pits and scratches in this part tended to affect all four sensors
equally. Indications are that when the surface irregularities are considerably
smaller than the dimensions of the probe the four sensors tend to produce different
background noise patterns and correlation techniques improve the signal to noise
ratio. When the surface irregularities are larger however, such as in the specimen
of Figure 26, the four sensors produce similar background noise patterns and corre-
lation is of no value. It should be noted that the specimen in question is actually
very rough and under most circumstances one would want to detect the conditions
which we have termed "surface roughness".

Equipment and Procedure

A diagram of the probe used in the eddy current correlation work appears in Figure
27. Figure 28 is a photograph of the probe and test part. The probe contains four
pairs of coils, A_1A_2, B_1B_2, C_1C_2, and D_1D_2. There is a separate bridge circuit
for each coil pair and the two coils of a given pair are incorporated into the
opposite arms of that bridge. Figure 29 shows the manner in which the coils are
electrically connected to the bridge circuitry. As discussed previously, each coil
pair acts like a set of differential coils contacting a slightly different portion of
the test part, and each acts as a source for one of the four signals available from
the probe. In general the signals have similar flaw responses and different back-
ground noise patterns and flaw clarity is improved upon taking a product.

Surface Profile (mils)

+1

-1

Position
on Part
(Inches)

1

18% Ni Steel

10 mil x 32 mil

4"

Scan Line

Longitudinal
EDM Slot

Transverse
EDM Slot

5"
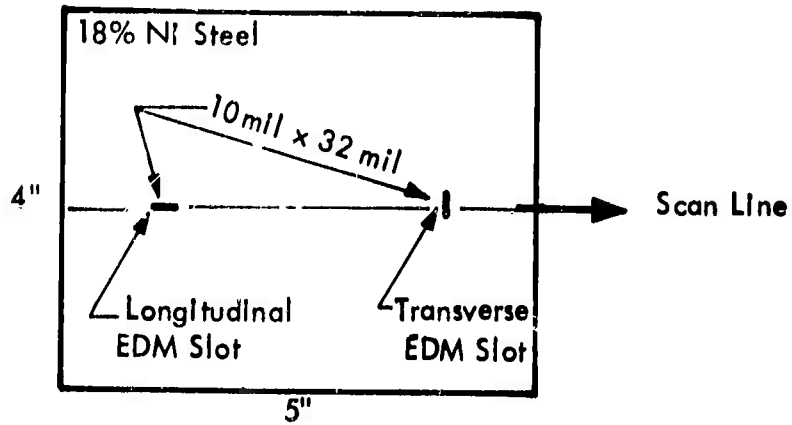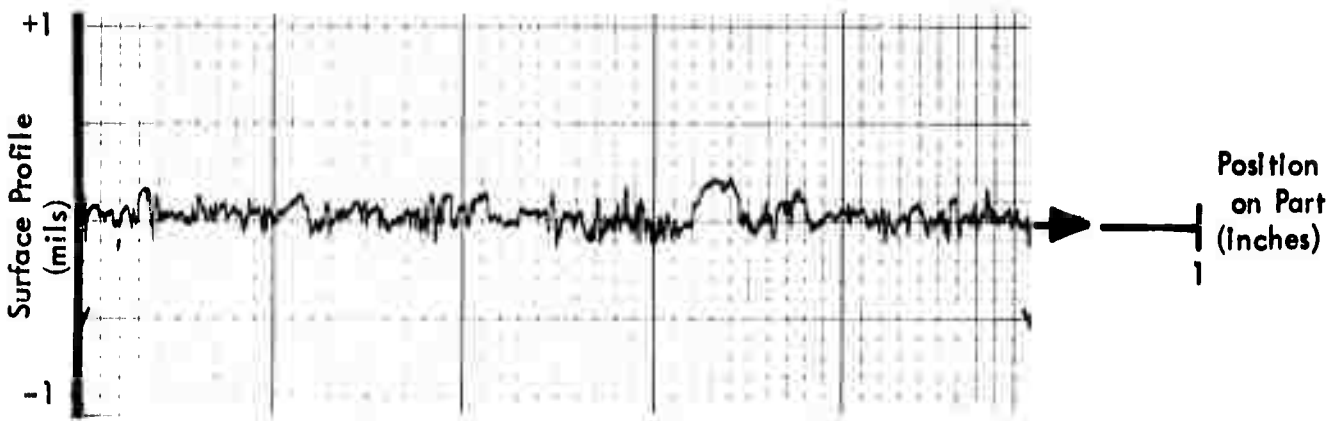
FIGURE 25   SMOOTH EDDY CURRENT TEST SPECIMEN
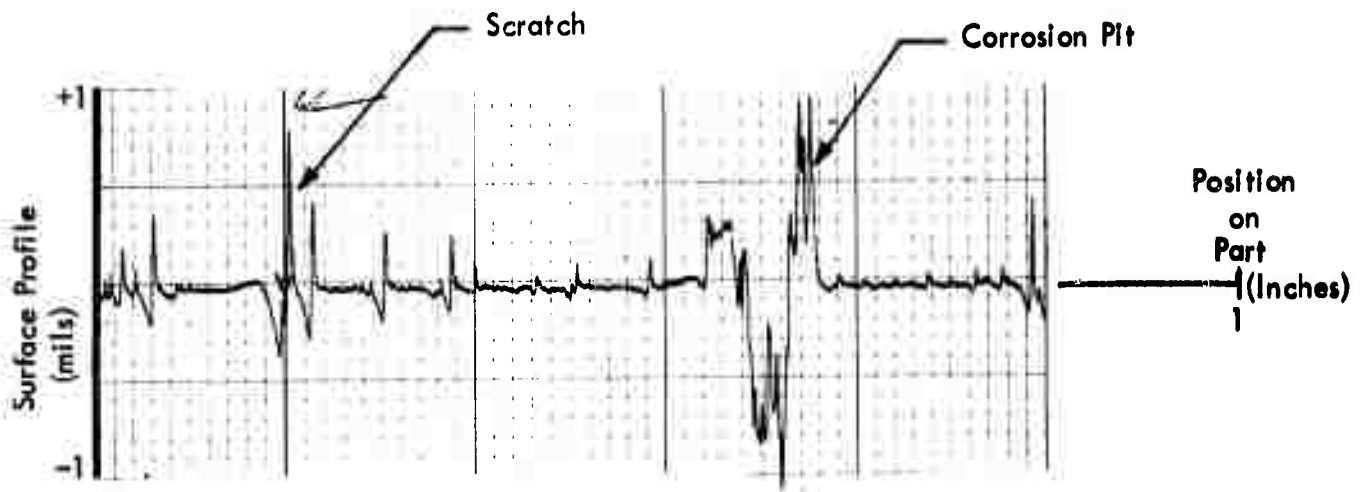
34

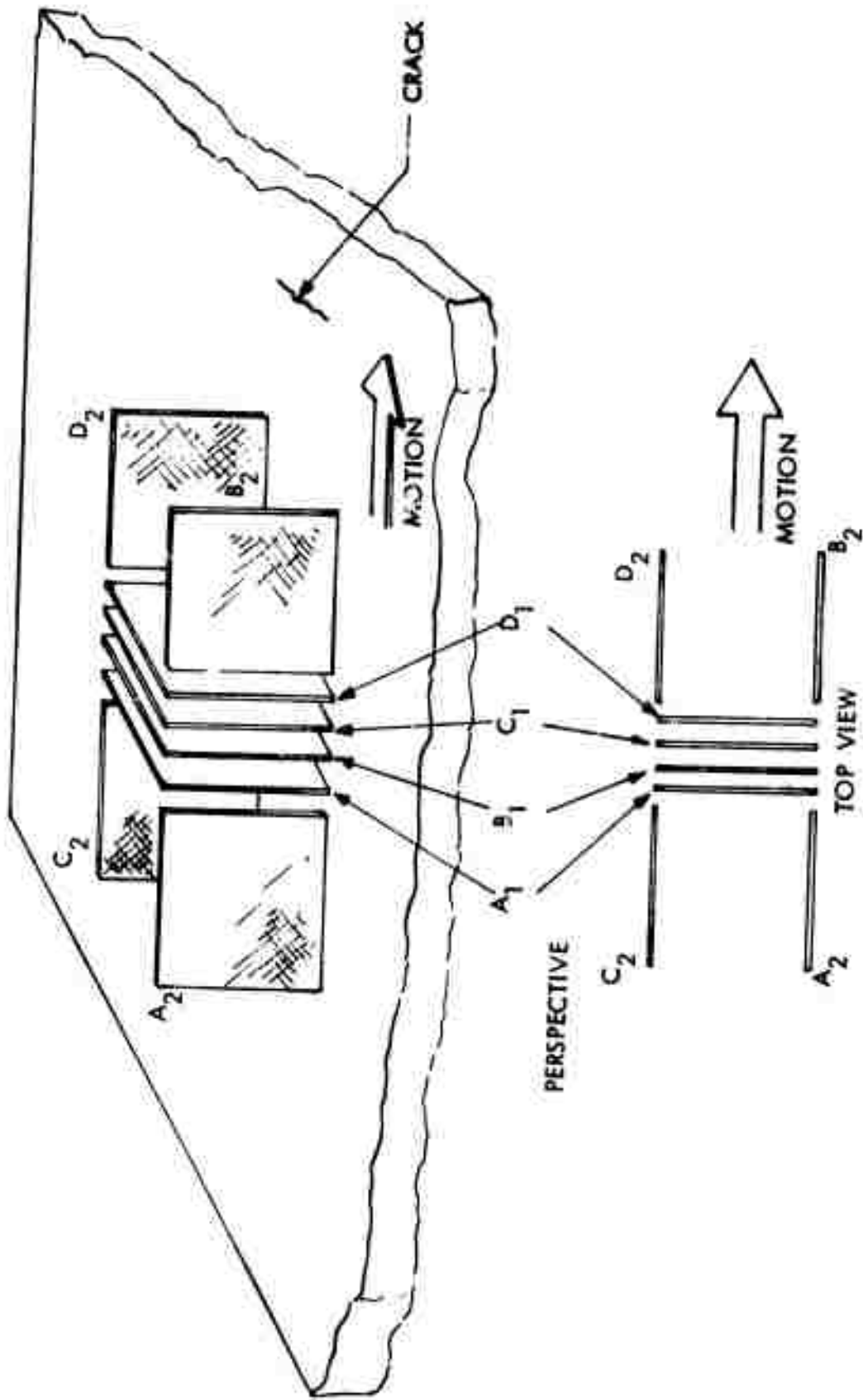FIGURE 26   ROUGH EDDY CURRENT TEST SPECIMEN
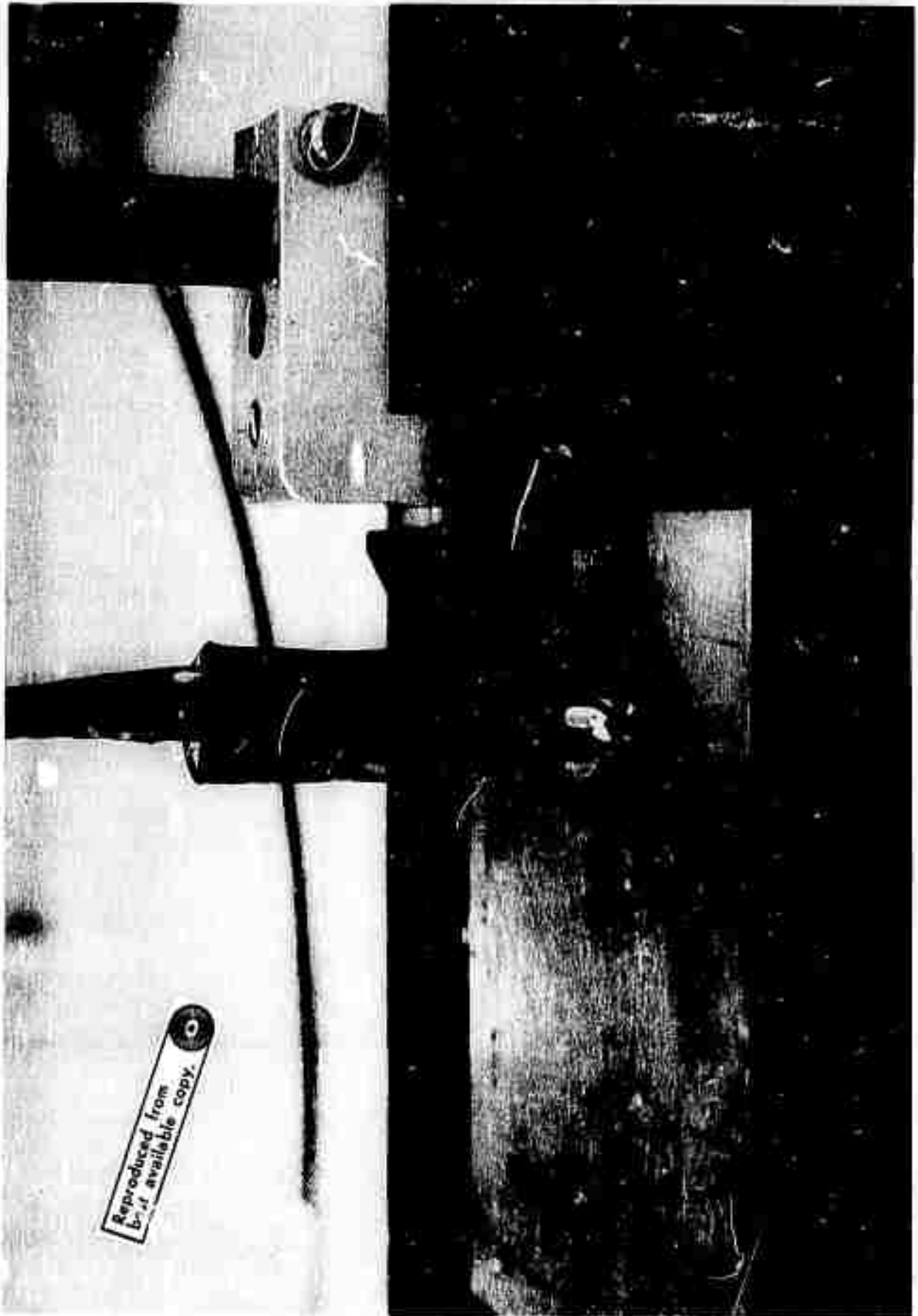
FIGURE 27 MULTIPLE COIL PROBE

36

FIGURE 28   PHOTOGRAPH OF PROBE AND TEST PART

The coils are square and are approximately two tenths of an inch on a side. Each coil consists of roughly ten turns of 5 mil copper wire. The crossbar of the "H" is that portion of the coil which produces a large response to sharp cracks. It consists of coils A_1, B_1, C_1 and D_1. These coils are not placed side by side as the diagram indicates. They are incorporated into a single quadrifiliar winding. This procedure insures that each coil contacts the part in an identical manner. Under these conditions the flaw indications occur in the four outputs at precisely the same time and there is no possibility of losing important responses as a result of the multiplication process.

The details of the bridge circuitry are shown in Figure 29. There are four bridges: one for each coil pair. The use of the potentiometer slide wire for the ground and signal output connections of the bridge assures that the power supply will see an approximately constant impedance during balancing. This frequently makes balancing easier. At first sight these circuits do not look like the conventional diamond shaped AC bridge, but they are equivalent electrically. They can be redrawn with the points P_1, P_2, P_3 and P_4 as the vertices of the diamond. This circuitry is commonly used in commercially available devices.

The four bridges are not completely independent. They have a common power supply and, due to the geometry of the probe, there is inductive coupling between coils in different bridges. As a result a balance adjustment in one bridge affects the state of balance in the other three bridges. It is not possible therefore to completely balance one bridge and then set about balancing the others. It is necessary to keep all four bridges in approximately the same state of balance at all times. This is done by partially balancing all four so that they have approximately the same output signal amplitude. This step is repeated, improving the balance but maintaining all output signals at the same reduced amplitude. A third repetition of this process generally produces adequate balance for crack detection. Although some care has to be taken in the balancing operation the interaction between the bridges is not a serious problem.

Figure 30 shows that data taken with the multiple coil probe is affected by the balance point if conventional amplitude detection is used. Data from one of the four coil pairs is shown. Oscilloscope traces of bridge outputs at three different balance points are shown at the top of the page. In each case the bridge balance potentiometers are adjusted differently. The physical location of the coil is the same for all cases and is indicated by the arrows in the data curves. Oscilloscope trace A is the bridge output when the coil is located at the position of the arrow in data curve A. This is similarly true for traces B and C. The test frequency is 100 KHz and the horizontal sweep on the oscilloscope is set at ten microseconds per division. The higher frequency components in the signal appear to be due to the second harmonic. Note that it is possible to completely lose a flaw signal if the bridge is not properly balanced. While it is possible to obtain an approximate balance condition for the four bridges by the procedures of the last paragraph it can be time consuming to balance with the

38
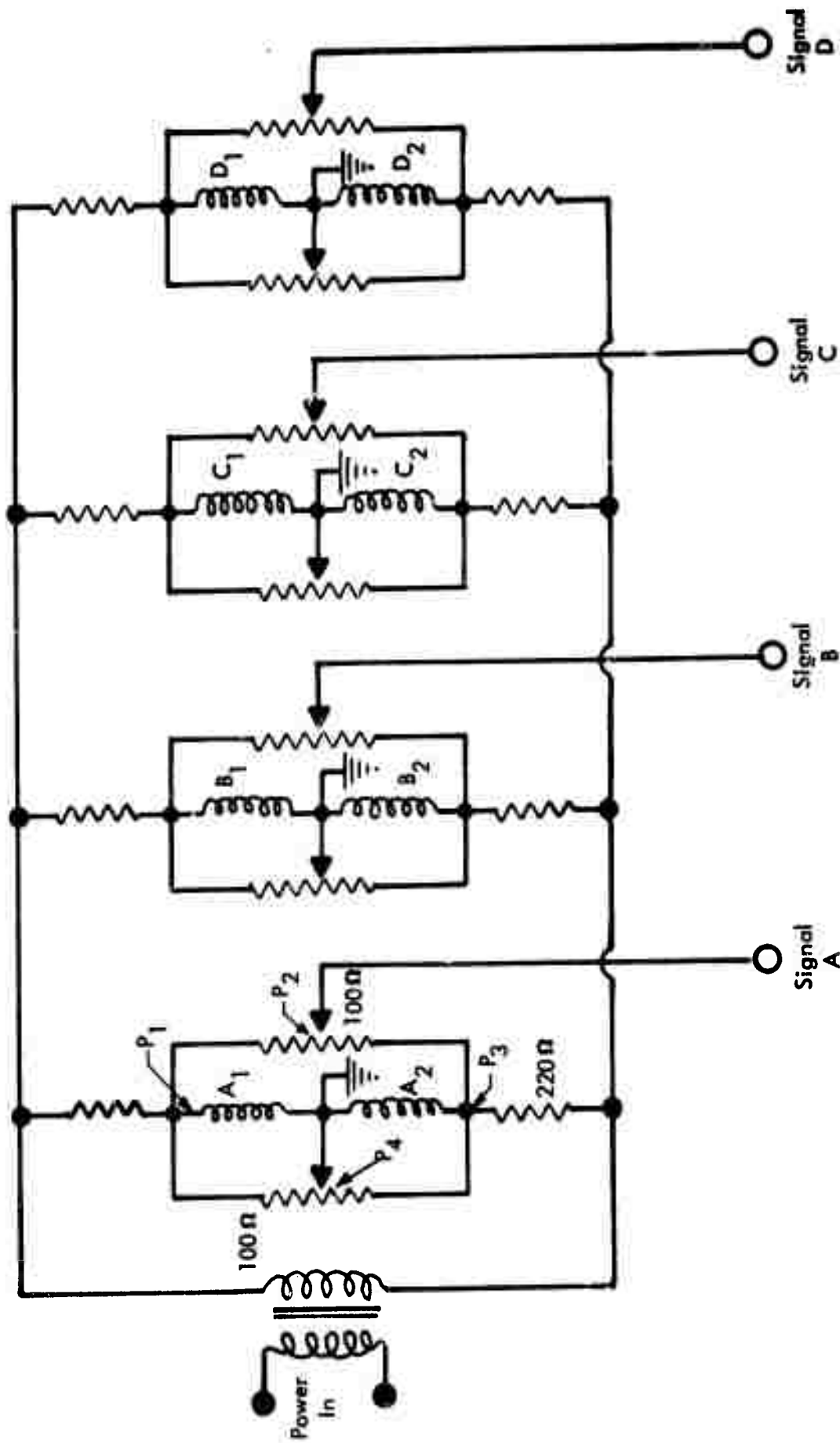
FIGURE 29 EDDY CURRENT BRIDGE
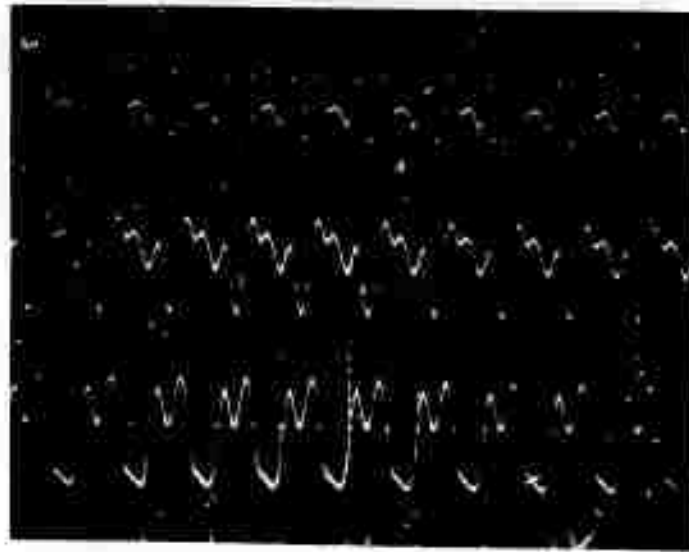
39

Amplified Bridge Output With Coil Located at Reference
Point
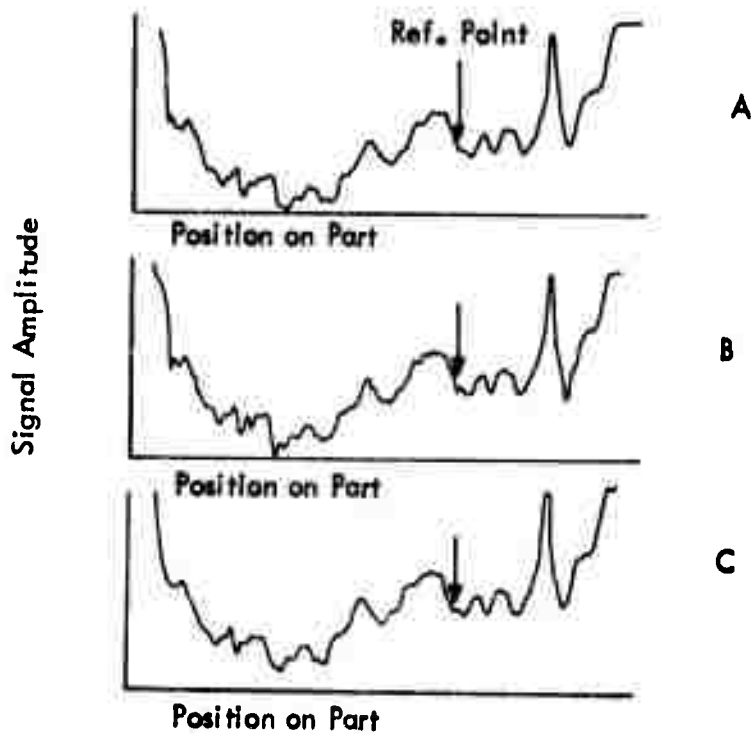
Pen Recordings of Scan Over Part

FIGURE 30   DATA OBTAINED USING AMPLITUDE SENSITIVE DEVICE OPERATING
AT THREE DIFFERENT BALANCE POINTS

Amplified Bridge Output With Coil Located at
Reference Point

Phase Detected Signal

Ref. Point

A

Position on Part

B

Position on Part

C

Position on Part
Pen Recordings of Scan Over Part

FIGURE 31   DATA OBTAINED USING PHASE SENSITIVE DEVICE OPERATING AT THREE
DIFFERENT BALANCE POINTS

41

precision indicated in Figure 30. This problem can be solved by using phase sensitive detection. Figure 31 shows that eddy current data is independent of balance point if phase sensitive detection is used. To obtain data of the type shown in Figure 31, one first obtains an approximate balance by conventional methods, and then adjusts the phase reference for maximum signal sensitivity. The latter step is straightforward with the multiple coil probe because the phase reference adjustments in the four channels are completely independent. Subsequent, moderate changes in balance point will not affect the output of the phase detected signal.

A rationale for the insensitivity to balance point of a phase detected signal is shown in Figure 32. The points 1 and 2 are balance points. The bridge is said to be balanced at point 1 if the balancing pots are so adjusted that the bridge output is zero when the eddy current coil assumes the impedance represented by 1. Point F represents the coil impedance when located directl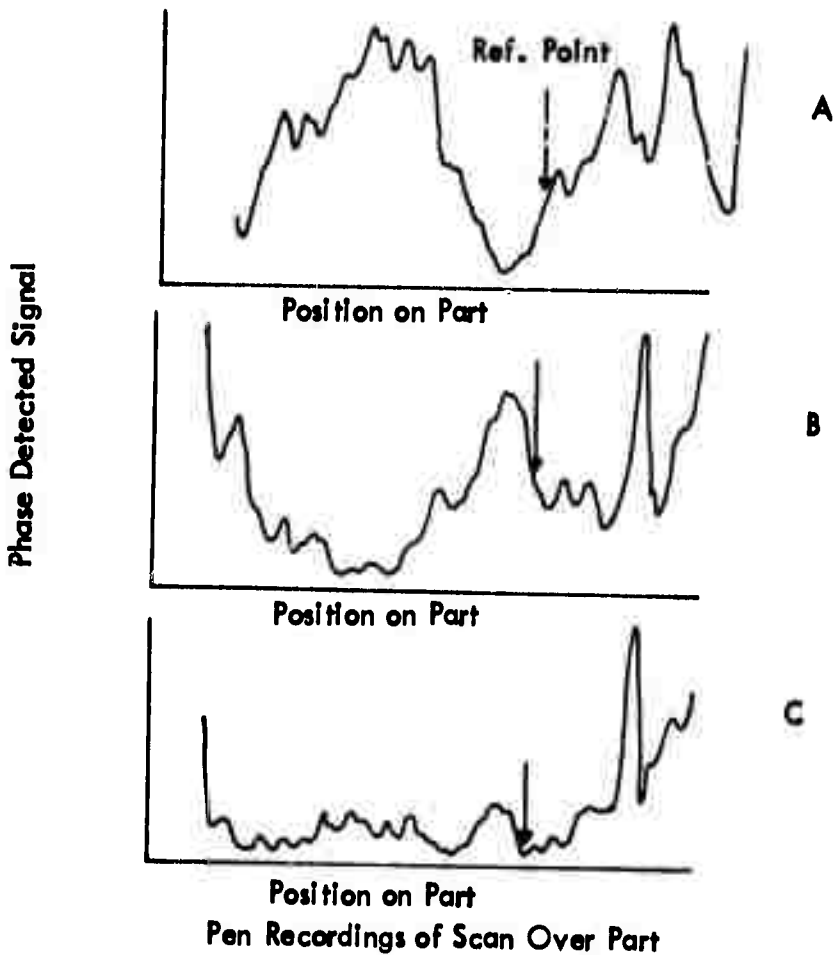y over the flaw and point N represents the coil impedance immediately adjacent to the flaw area. In the upper two diagrams the point 0 is the intersection of the line dropped from the balance point to the line NF extended. The output of the amplitude sensitive device is proportional to the magnitudes of the various vectors shown. As the diagram indicates the response of the instrument as the coil passes from a non-flaw area to a flaw area is dependent upon balance point. In fact, in one case the needle will go up scale and in the other case down scale. The output of the phase sensitive device, rather than being proportional to vector magnitudes, is proportional to the components of vectors in a given direction. The components in the direction of the flaw response are shown in the upper two diagrams of Figure 32. As the diagrams indicate, the flaw response is independent of balance point. In fact, in every case the flaw response is precisely the vector NF. Although the numbers shown are in arbitrary units, the results can be verified by measuring the various vector lengths with a ruler.

Figure 33 is a block diagram of the electronics as a whole. A photograph of the electronics appears in Figure 34. Four HR-8 lock-in amplifiers are used. One acts as a signal generator and detector. The other three are synchronized to it and are used only for phase sensitive detection. The driver line passes from the oscillator to a power amplifier and then to the bridges. The four bridge outputs are fed to the four lock-in amplifier inputs. After amplification and phase detection four signals, A, B, C, and D, are obtained. These final outputs are essentially DC signals which vary as the eddy current probe scans along the part. Although not shown in the diagram these outputs can be connected to an XY plotter for direct recording or they can be connected to the inputs of the multiplier shown in Figure 35.

The multiplier differentiates each signal and then performs a quadruple product as indicated in the diagram. It is necessary to differentiate the signals A, B, C, and D so that they differ from zero only when the coils are responding to a sharp discontinuity. This assures that the product A x B x C x D will be non-zero only when sharp responses occur simultaneously in all four channels. Without differentiation the multiplication process would not effectively reduce background noise. As can be seen from the diagram the quadruple product was formed by interconnecting three analog multiplier units.

42

$V = \overline{OF} - \overline{ON} = -26 - (-42) = +16$ Units

$V = \overline{OF} - \overline{ON} = 25 - 9 = +16$ Units

Phase Sensitive Instrument

1, 2 = Bridge Balance Points

F = Flaw Response

N = Nonflaw Response

$V = \overline{1F} - \overline{1N} = 29 - 44 = -15$ Units

$V = \overline{2F} - \overline{2N} = 29 - 17 = +12$ Units
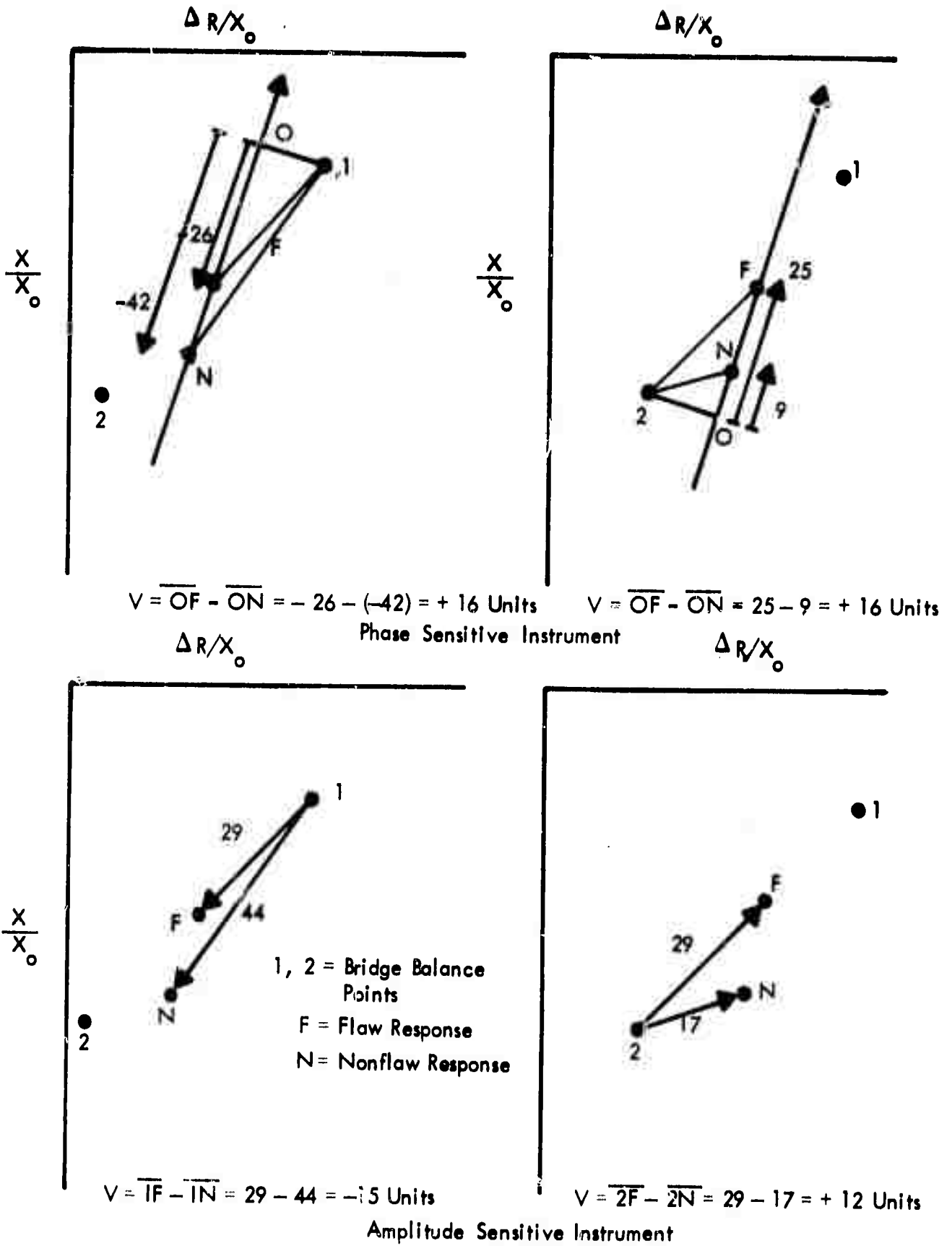
Amplitude Sensitive Instrument

FIGURE 32   REACTION OF AMPLITUDE AND PHASE SENSITIVE
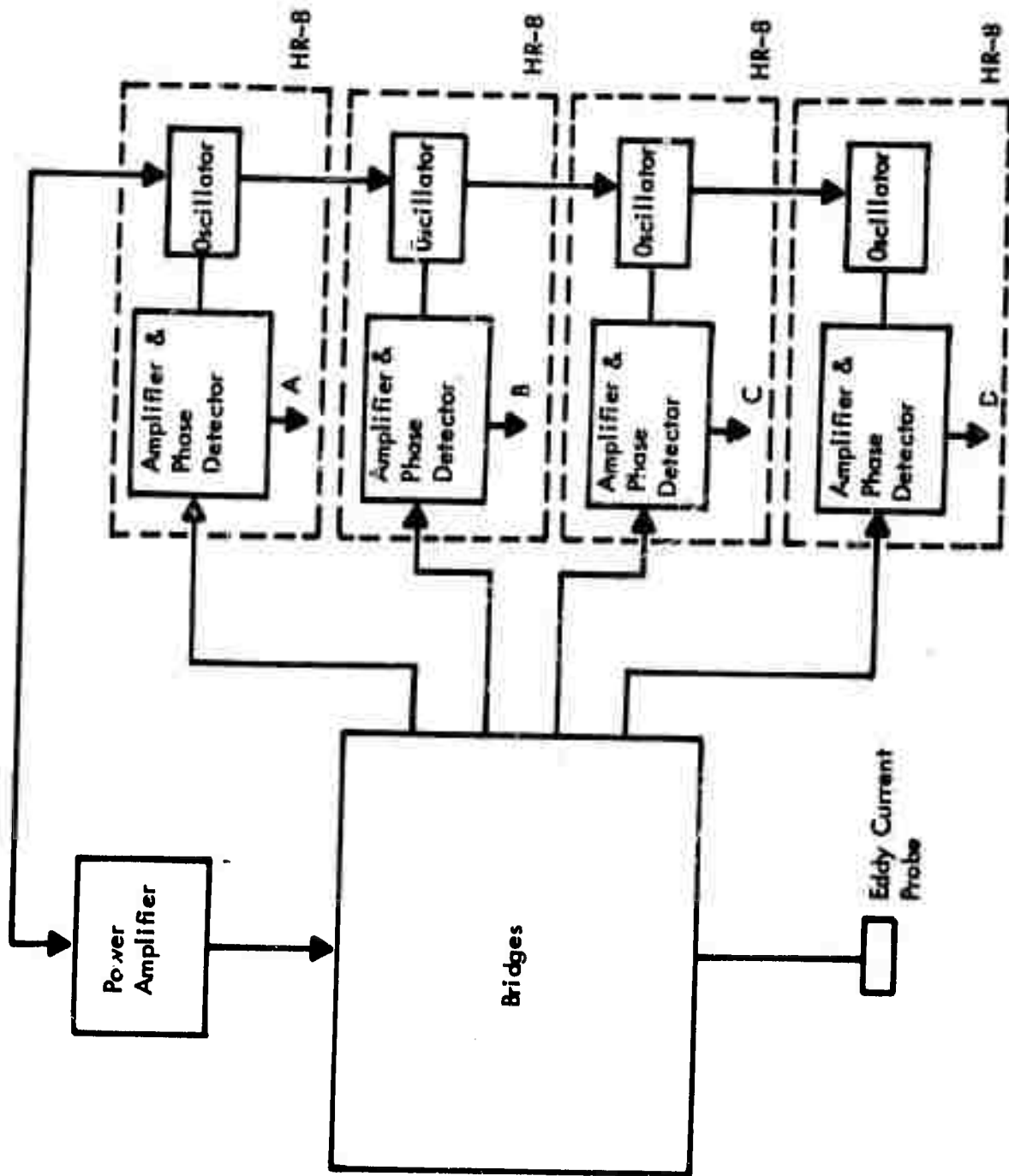DEVICES TO A CHANGE IN BALANCE POINT

43

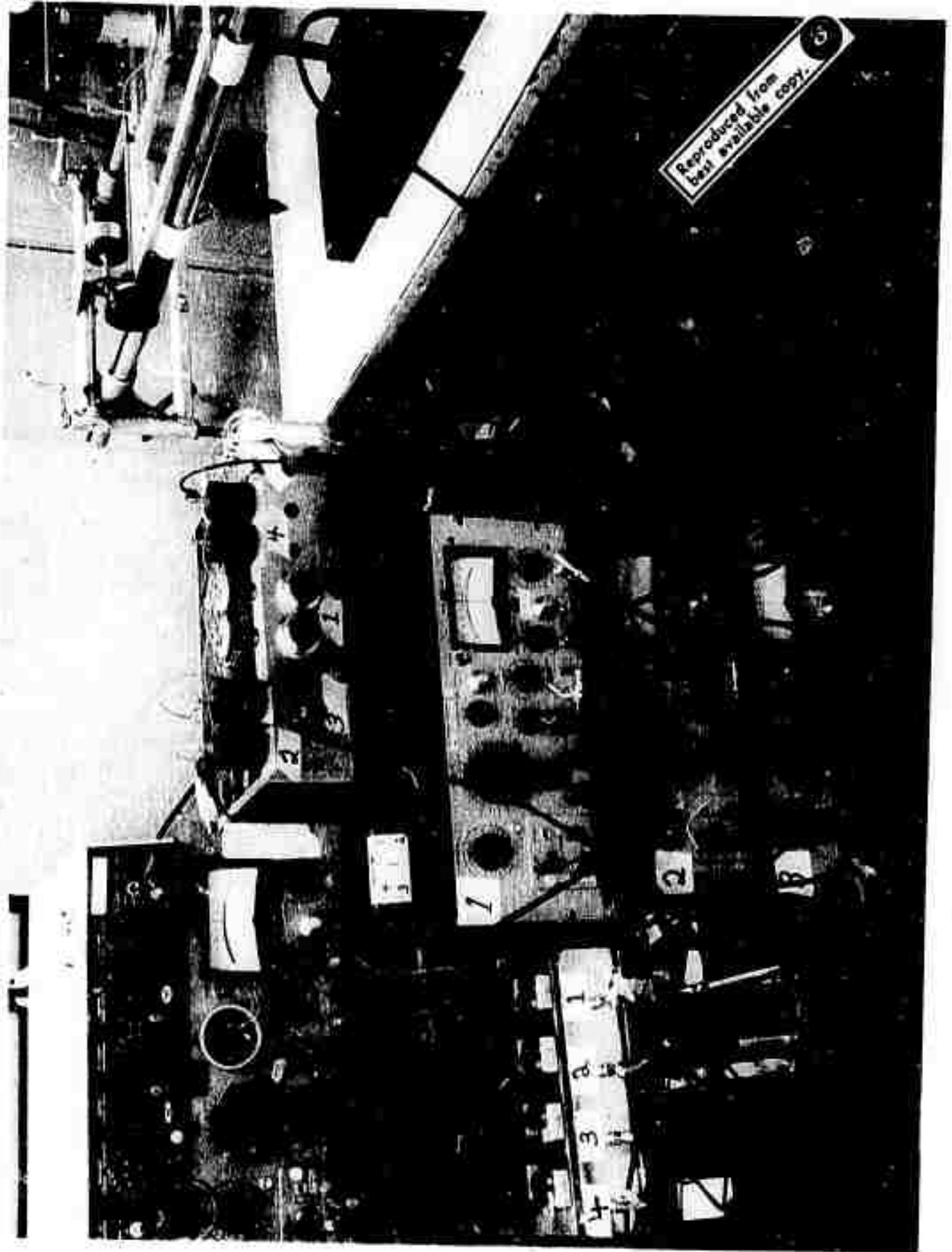FIGURE 33   BLOCK DIAGRAM OF EQUIPMENT USED FOR REAL TIME MULTIPLICATION OF EDDY CURRENT CRACK DETECTION DATA
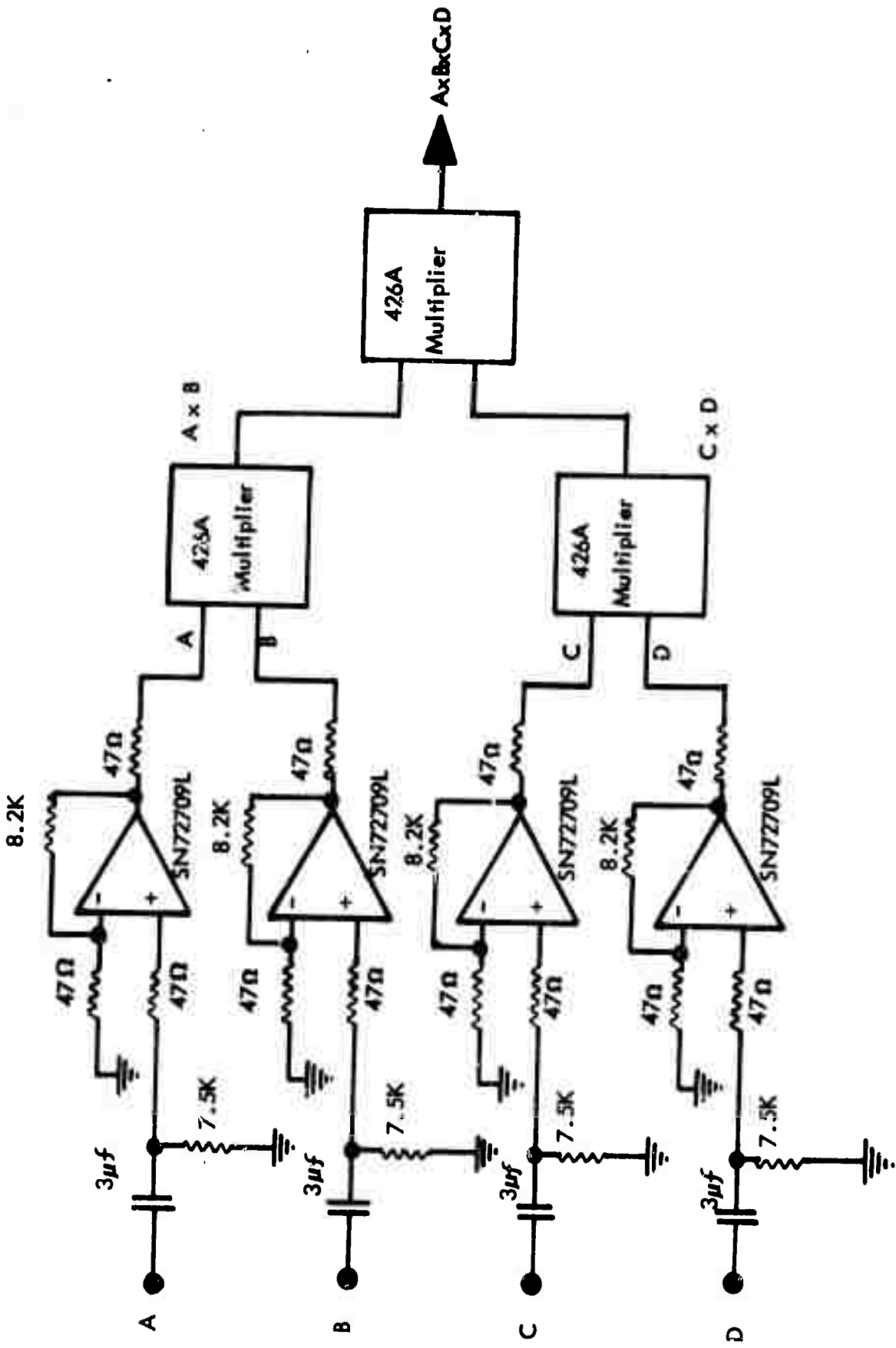
44

FIGURE 34   PHOTOGRAPH OF EDDY CURRENT ELECTRONICS

FIGURE 35   MULTIPLIER CIRCUITRY

46

Data and Conclusions

The test part of Figure 25 was inspected using the multiple coil eddy current probe. The probe scanned along the line indicated in that figure. Each of the four signals A, B, C, and D appearing at the lock-in amplifier outputs was recorded on an XY plotter. The results are shown in Figure 36. Notice that all four curves contain indications from the EDM slots. The transverse slot at the right end of the plate produces a narrow positive pulse in each channel. The slot parallel to the probe motion at the left end of the part produces a narrow negative pulse in each channel. The curves are in general different in the non-flaw regions of the part, but the background noise patterns do not differ as much as the ultrasonic noise patterns discussed earlier in the report. It is for this reason that four channels are being examined rather than three. Curves C and D, for instance, contain several positive excursions in common. Curves A and B have several negative excursions in common. The binary products A x B and C x D will not therefore remove all of the significant background noise. Those binary products can be seen in the two top curves of Figure 37. The major peaks here are all positive because both the positive and negative peaks in the original data have experienced algebraic multiplication. A detailed examination of the data will convince the reader that the binary product curves are indeed obtained by multiplication of the raw data curves. The final quadruple product A x B x C x D appears in the bottom curve of Figure 37. Notice that the signal to noise ratio is significantly better in the final product curve than in any of the original data curves. The two major peaks remaining are due to the EDM slots, and all large peaks from flaw free areas have been removed.

Data obtained from the same test part using commercially available eddy current instruments appears in Figures 38 and 39. Indications from both of the EDM slots can be located in these curves but there are a number of other indications from non-flaw conditions which are equally as large. The flaw clarity is approximately the same as that observed with the multiple coil probe prior to multiplication of the data. The crack indications are not as clear as those appearing in the quadruple product data. It is important to note that the effective working area of the coil used to produce the curves of Figures 38 and 39 is the same as that of the multiple coil probe. Data comparisons between coils of differing size is misleading. Although a small coil may be more sensitive to cracks, it inspects a small area, and many scans may be necessary to examine a given region on a part. The effective width of all of the probes discussed in the present work is approximately two tenths of an inch.

OPTICAL PROCESSING OF X-RAY RADIOGRAPHS

Theory

A brief study has been made of the coherent optical processing of x-ray radiographs. Attempts have been made to enhance marginally visible crack indications and to provide a quantitative measure for weld porosity. Fairly well established optical techniques have been employed. For a detailed discussion of these techniques one can refer to a number of texts[4, 5].
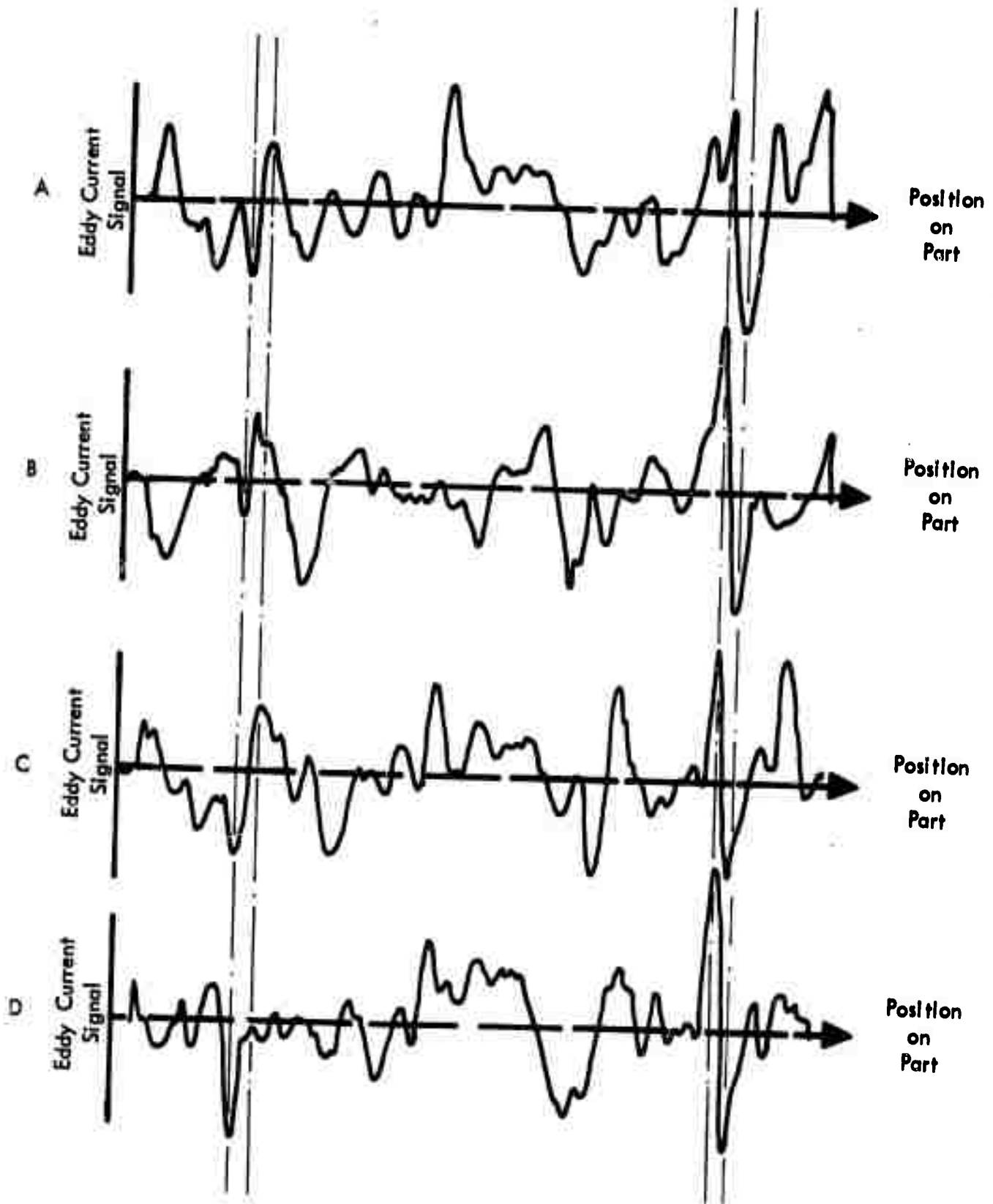
FIGURE 36   EDDY CURRENT INSPECTION DATA PRIOR TO MULTIPLICATION
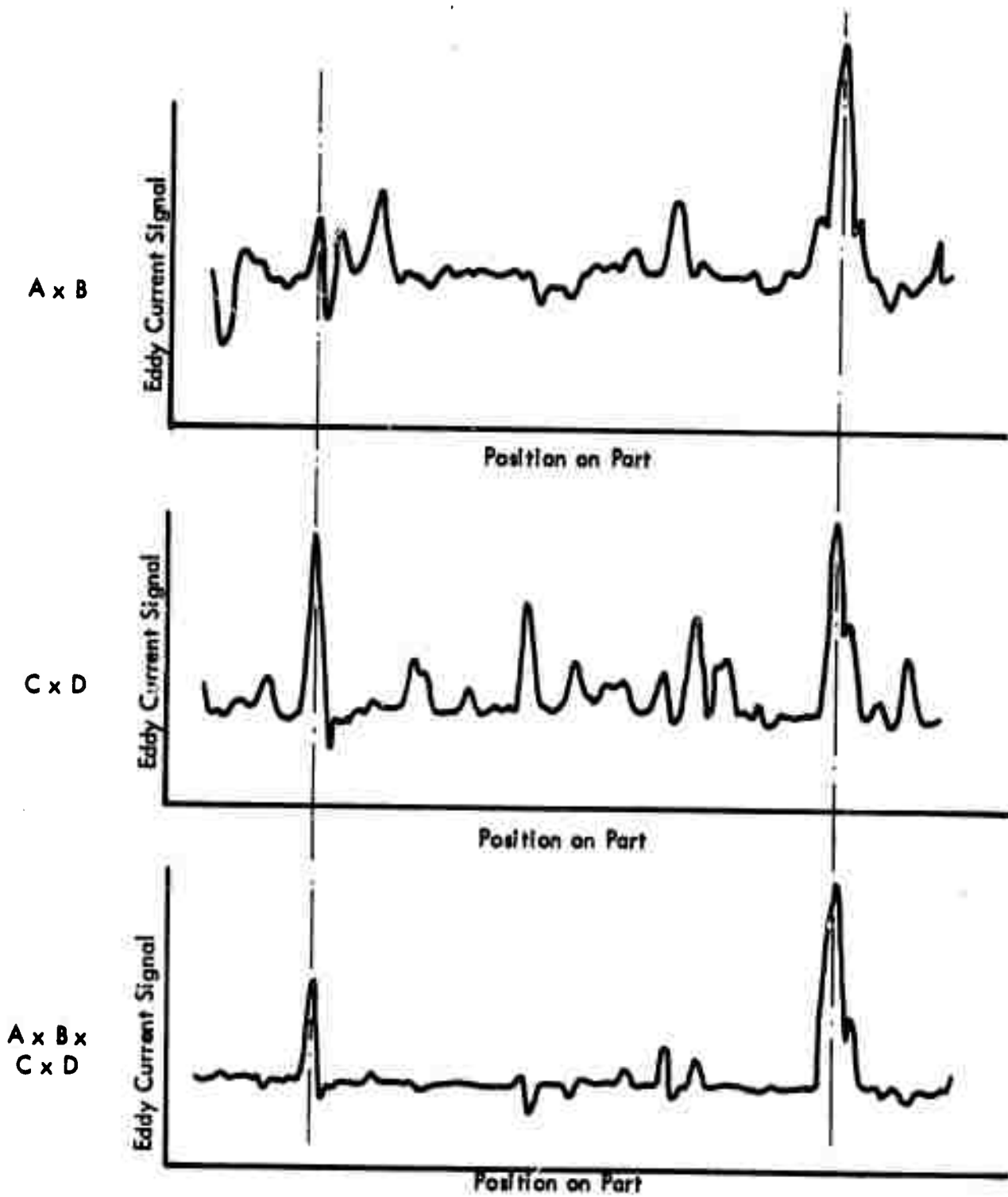
48

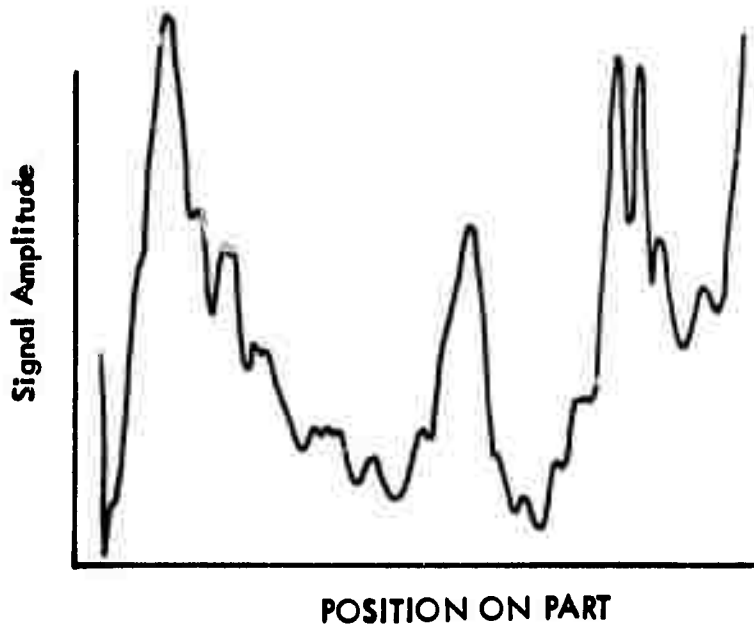FIGURE 37   REAL TIME PRODUCTS OF EDDY CURRENT DATA

FIGURE 38   DATA OBTAINED WITH COMMERCIALLY AVAILABLE AMPLITUDE
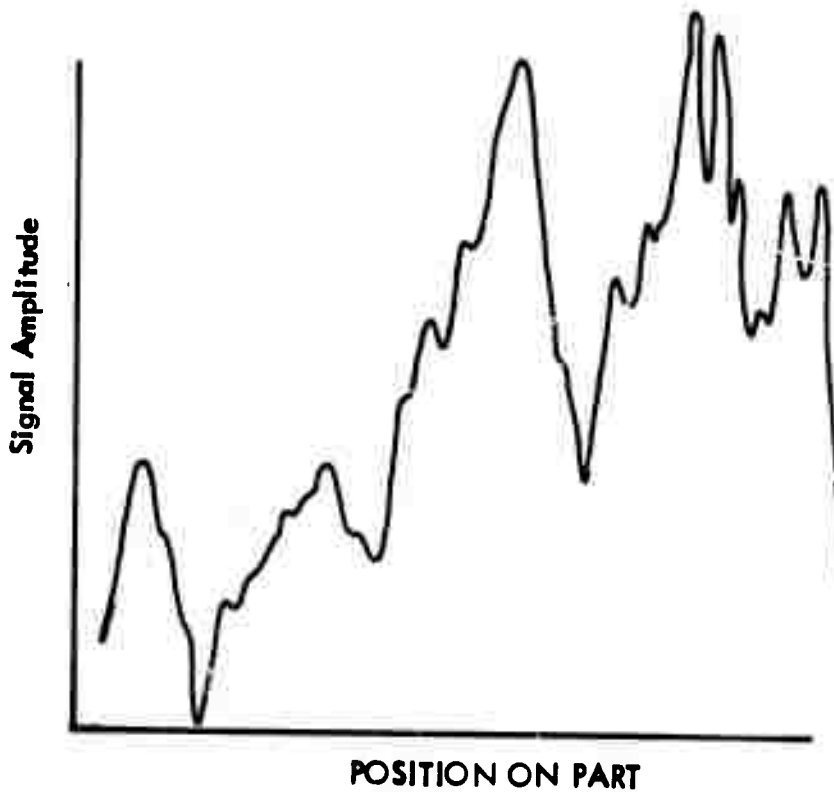SENSITIVE EDDY CURRENT INSTRUMENT

FIGURE 39   DATA OBTAINED WITH COMMERCIALLY AVAILABLE PHASE SENSITIVE
EDDY CURRENT INSTRUMENT

50

Simple spacial filtering can be performed by putting stops of an appropriate shape into the frequency plane of certain optical systems. We have attempted to enhance the contrast of high frequency crack indications by removing low frequency noise with wire and knife edge filters. A number of exposures have been made of marginally visible, frequency filtered crack indications. The results have not been encouraging. Photographic enhancement techniques which make use of film characteristics appear to be simpler and more effective.

The light distribution in the frequency plane of certain optical systems is the two dimensional fourier transform of the transparency inserted into the input plane. We have used this fact to examine the fourier transform of weld porosity indications. The transform is an average of the porosity indications over an area of about one square inch and is a potential measure of the severity of the porosity. We have recorded transforms on film by making exposures in the frequency plane. Again the results have not been promising. Low spatial frequencies and lack of contrast in the porosity indications significantly reduced the quality of the transforms.

Automatic detection or categorization of crack indications on X-ray film is an area in which optical processing may be of value. Experiments involving automatic detection were planned but we have been unable to pursue them to completion. Although the optical experiments have not been successful several interesting attempts have been made and the details are presented in the sections to follow.

OPTICAL FILTERING OF RADIOGRAPHIC FLAW INDICATIONS

Specimens

Spatial filtering studies were performed on a set of radiographic negatives produced from artificial crack standards. The negatives contained indications several mils wide, varying in clarity from high contrast to less than 1 percent contrast. All of the crack indications were several inches long and the average background density of the radiographs was 1.35 to 1.45. The negatives were type M double emulsion film.

Spatial filtering studies were also performed on a negative produced from an electron beam welded tensile specimen. This specimen contained lack of fusion in an area in which filler material had been added to the weld. The crack image on the X-ray negative is visible under magnification, but only with difficulty. The crack is made harder to see by the presence of the image of the filler material which had a higher atomic number than the base metal. The filler image is, however, somewhat broader than the crack image and spatial frequency filtering was employed in an attempt to enhance the crack indication. Due to the low contrast and small size of the indications involved it was not possible to provide useful reproductions for the report, but the procedure and results are discussed below.

Equipment and Procedure

Figure 40 is a diagram of the equipment used for the spatial filtering studies. A photograph of the equipment can be seen in Figure 41. The light source is a Spectra Physics He-Ne laser. A one inch diameter coherent beam of reasonably uniform intensity is obtained through the use of a Spectra Physics spatial filter. The filter contains a condenser, a 10 micron pinhole, and a collimator. The radiographs to be processed are inserted into the input plane, several inches in front of the collimator, and are illuminated by the coherent light beam. The transform lens is a coated achromat with a diameter of 66.0mm and a focal length of 195.0mm. The spatial filtering is performed in the back focal plane of the transform lens. A photograph of the knife edge filter can be seen in Figure 42. The knife edge is mounted on a precision adjustment X, Y stage. When in use the X, Y stage is mounted in the optical system in such a manner that it can be easily adjusted in and out of the focal plane. Other filters were constructed by extending fine wires across the circular opening in the X, Y stage. The wires were from 1 to 10 mils in diameter. An inverse transform lens is not used to produce an image of the filtered transparency. It was found that an adequately focussed exposure could be obtained without such a lens by proper placement of the film pack. The conventional lens law was used to determine the relative locations of the input transparency, the transform lens, and the Polaroid film pack. A high contrast test pattern was used to verify focus. Exposure times were controlled by a shutter placed between the laser and the condensing lens.

Data and Conclusions

The artificial crack specimens were processed using the wire filters. The wires were used to block out the DC component of the diffracted light. This component is produced by the uniform background on the radiographic negative. The light diffracted by the crack indication was able to pass around the wire filter and was blocked to a lesser extent. A slight contrast enhancement was observed. However, contrast improvements using non-coherent photographic enhancement techniques appear to be simpler and more effective[6].

The electron beam welded tensile specimen was processed using the knife edge filter. Careful placement of the filter removed all noise of low spatial frequency including the filler indication. The crack indication, which was typically several tenths of a mil wide was retained. Nevertheless the filtered transparency was not superior to the original. With the low frequency information gone, the environment in which the crack occurs is no longer visible. There is greater uncertainty about the nature of the indication on the filtered transparency than on the original radiograph. It is not likely that the filtering process will reveal cracks which are totally invisible in the initial negative. The filtering process does not appear to result in useful improvements.

52

He –Ne
LASER

Spectra
Physics
Spatial
Filter

Input
Transparency

Collimator

Condenser
10µ Pinhole

Transform Lens

Knife Edge
Filter

Polaroid Film Pack

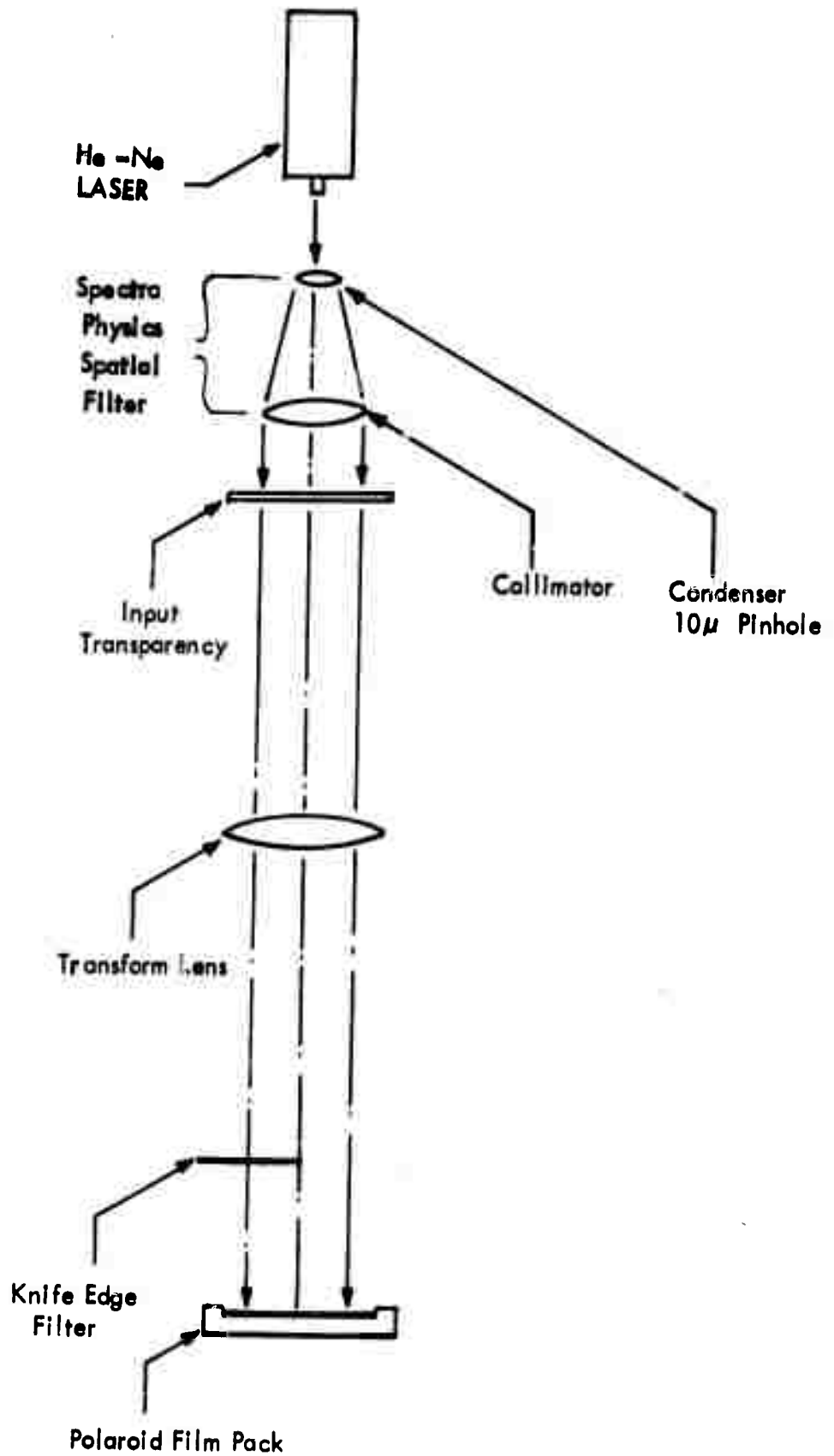FIGURE 40   DIAGRAM OF EQUIPMENT USED FOR OPTICAL FILTERING
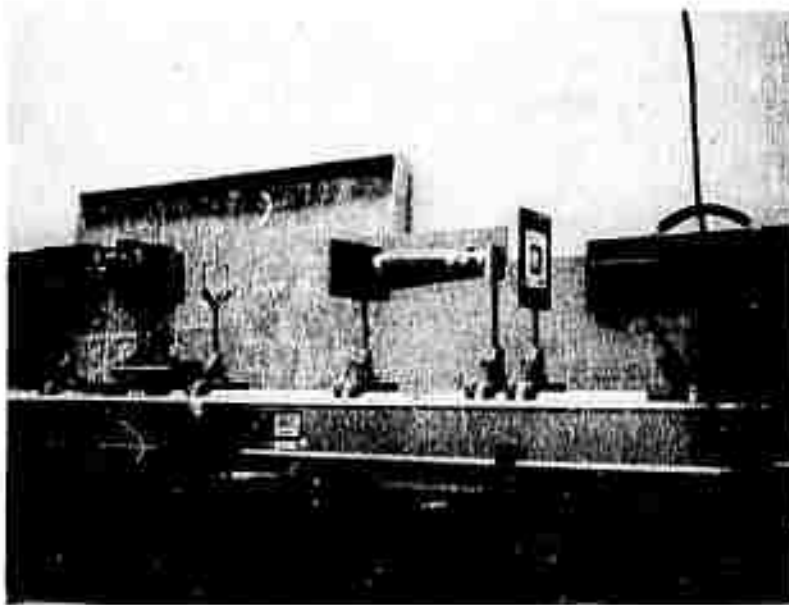OF RADIOGRAPHIC NEGATIVES

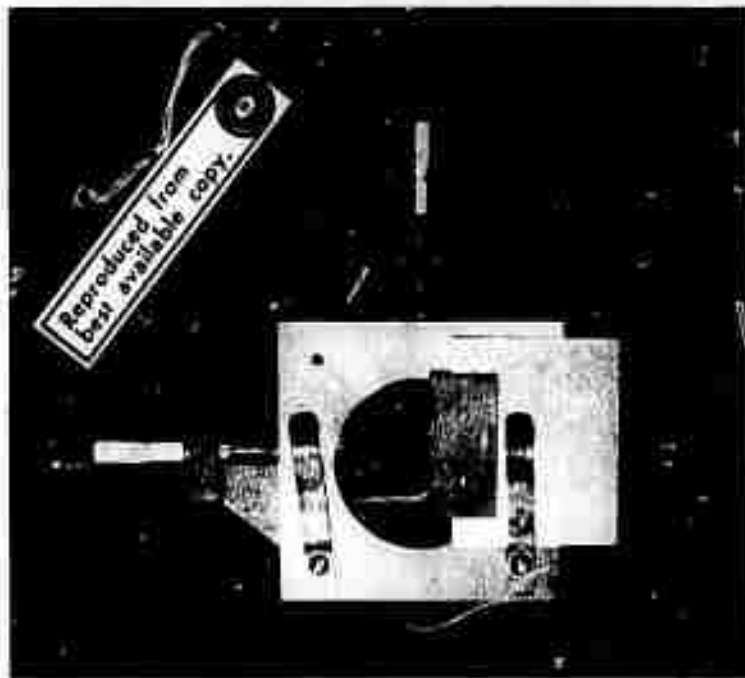FIGURE 41   OPTICAL FILTERING EQUIPMENT

FIGURE 42   OPTICAL FILTER

FOURIER TRANSFORM OF WELD POROSITY INDICATIONS

Specimens

The fourier transform studies were performed using the ASTM porosity standards.
These standards are available in the form of radiographic negatives. Typical
fine porosity and coarse porosity indications were selected for observation.
Prints made from the actual negatives used appear in Figures 43 and 44.

Equipment and Procedure

A diagram of the equipment used is shown in Figure 45. From the light source to
the transform lens the equipment is identical to that described in the previous sec-
tion. The fourier transform of the information on the input transparency appears at
the back focal plane of the transform lens. A second lens has been used to reimage
the transform plane with a magnification of ten. A film pack located behind the
second lens was used to record the enlarged fourier transform patterns.

Data and Results

It is not possible to transform the porosity indications directly because the spatial
frequencies involved are too low. All of the interesting information is lost in the
bright central spot. An attempt was made to scatter the useful information away
from the central spot by inserting a fine screen into the input plane. The fourier
transform of the screen in the absence of porosity is shown in Figure 46. This trans-
form was recorded on film, in actual size, and a negative was prepared for use as a
spatial filter. The filter was mounted on the X, Y stage and placed in the fourier
transform plane. With the screen in the input plane the filter perfectly matches the
light intensity distribution in the transform plane and was placed so that most of
this light is removed from the beam. The filtered fourier transform pattern is shown
in Figure 47. Figures 48 and 49 show the filtered transform pattern with the fine and
coarse porosity standards inserted in the input plane. The photographs should be
compared by selecting one of the points produced by the fine screen and examining
the light scattered about that point. There is a very slight difference between the
transform patterns but certainly not enough to provide a quantitative differentiation.

In a second set of experiments, the low frequency porosity information was converted
to a higher frequency by forming photographic reductions of original negatives. This
operation increased all frequencies by a factor of five. The original one square inch
sample was reduced to a small square one fifth of an inch across. In order to make
full use of the one square inch coherent beam the reduced image was repeated in the
square array shown in Figure 50. Although each element of the square array is
identical in the present photographs, each small square could presumably be taken
from a different portion of the weld. The fourier transform would then represent an
average of all of the information included on the transparency. Reductions were also
made of an optical test pattern as a check on system performance. The reduced test
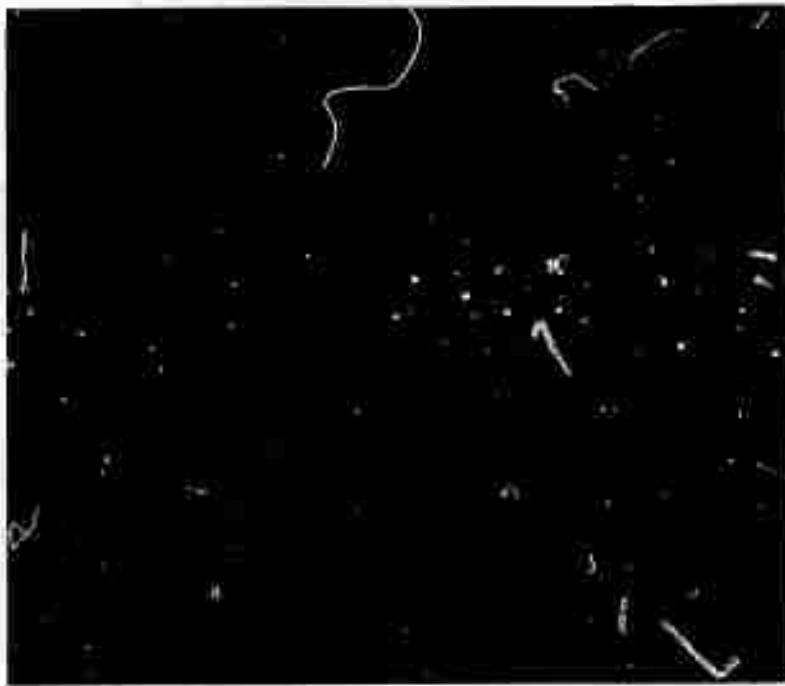
FIGURE 43   ASTM FINE POROSITY STANDARD

FIGURE 44   ASTM COARSE POROSITY STANDARD

He –Ne LASER

Spectra
Physics
Spatial
Filter

Collimator

Condenser
10 μ Pinhole

Input
Transparency

Transform Plane

Transform
Lens

Imaging Lens

Polaroid
Film Pack

FIGURE 45   DIAGRAM OF EQUIPMENT USED FOR OBTAINING
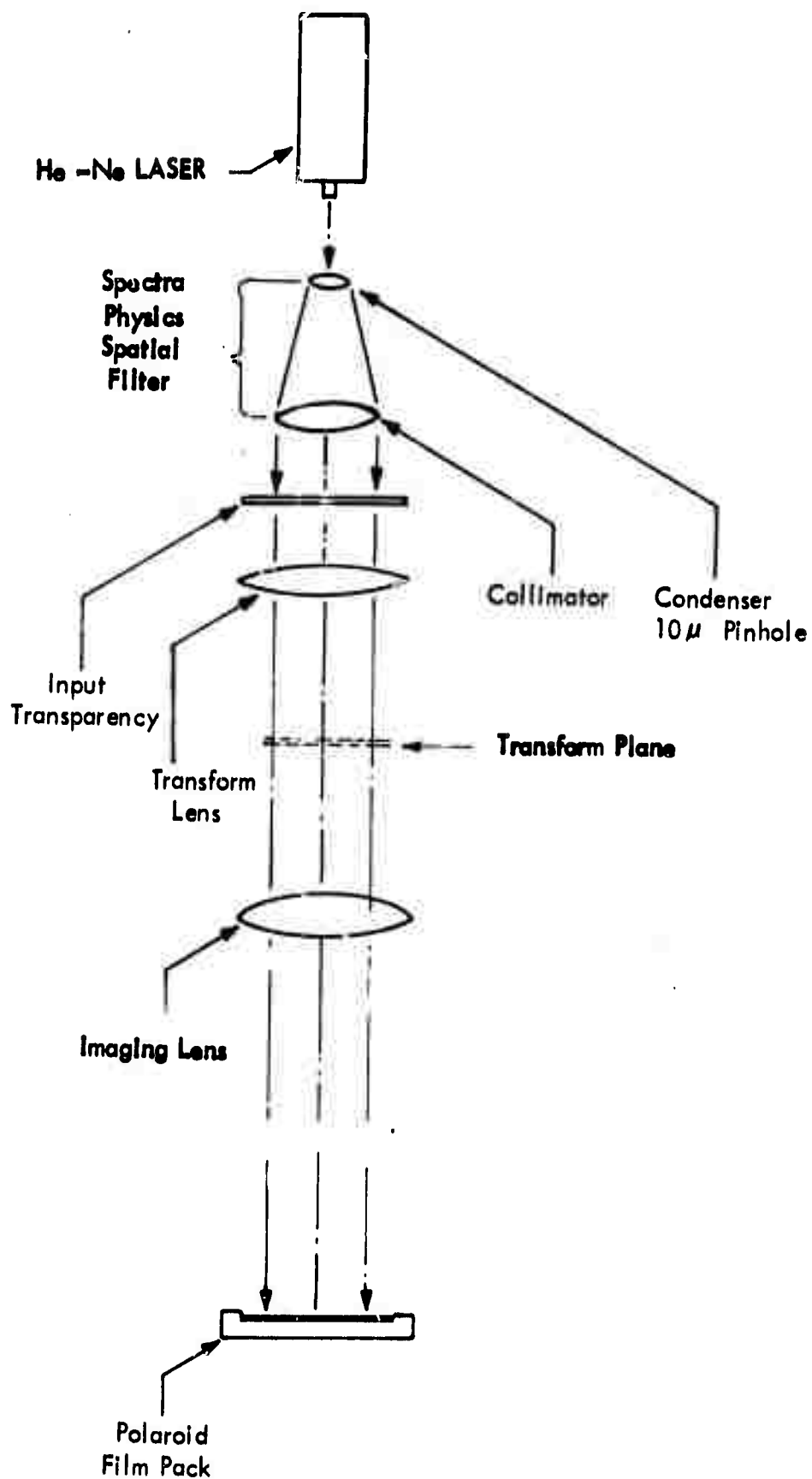FOURIER TRANSFORM OF RADIOGRAPHIC POROSITY INDICATIONS
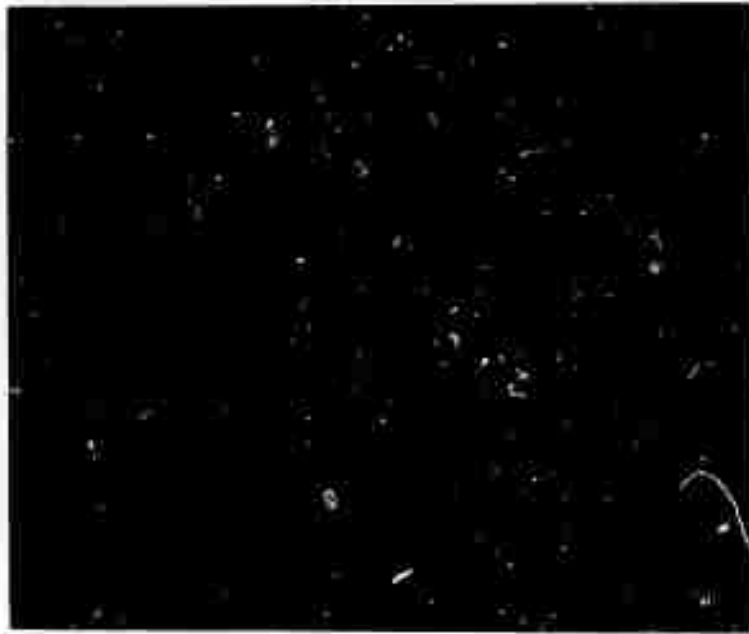
57

FIGURE 46   FOURIER TRANSFORM OF SCREEN

FIGURE 47   FILTERED TRANSFORM PATTERN IN THE ABSENCE
OF POROSITY

FIGURE 48   FILTERED TRANSFORM PATTERN FOR FINE POROSITY

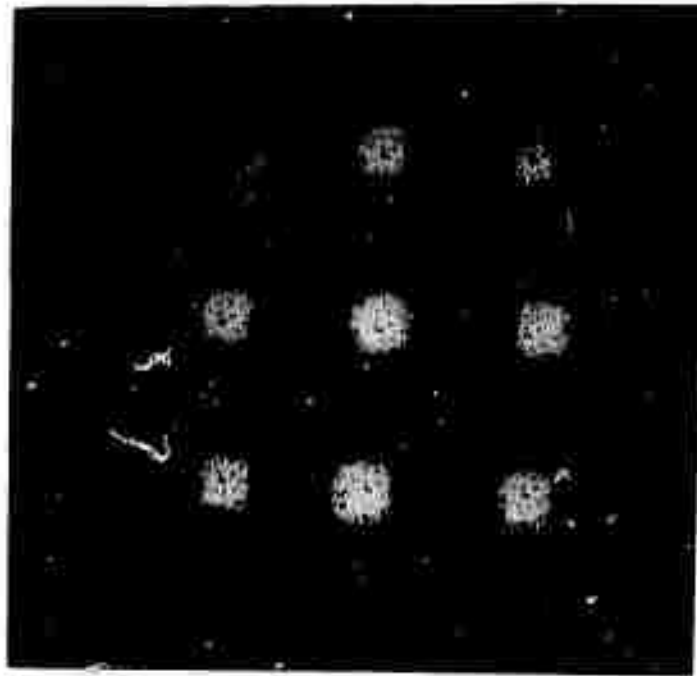FIGURE 49   FILTERED TRANSFORM PATTERN FOR COARSE POROSITY

FIGURE 50   REDUCED FINE POROSITY FORMAT
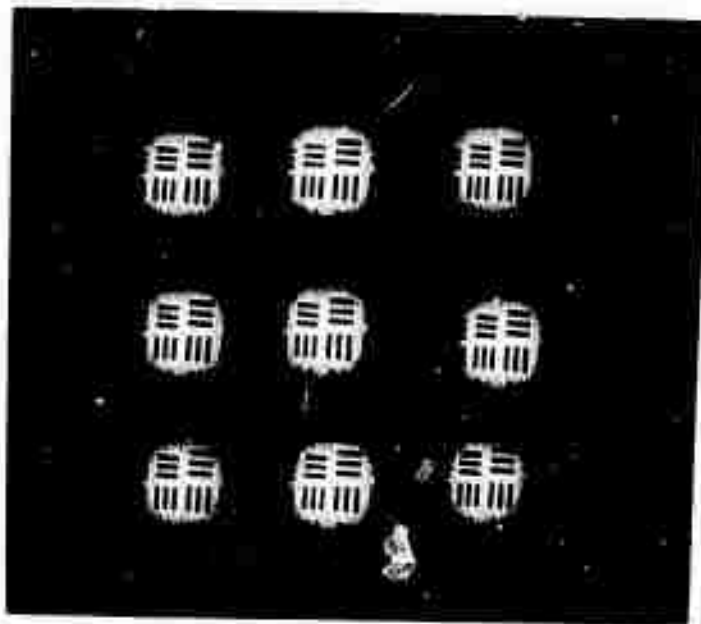
FIGURE 51   REDUCED TEST PATTERN FORMAT

pattern format is shown in Figure 51. For comparison purposes, a porosity free region on one of the ASTM standards was reduced and recorded in a similar square array.

The fourier transform of the porosity free region is shown in Figure 52. Figures 53 and 54 show the fourier transform of the test pattern and the fine porosity. The appearance of the test pattern transform indicates that the optics are performing as expected. A porosity transform is beginning to appear but it has almost no structure and it does not appear likely that these techniques will result in a quantitative measure of porosity. The low quality porosity transforms are almost certainly due to the moderate contrast existing on the original negatives.

FIGURE 52 FOURIER TRANSFORM IN THE ABSENCE OF POROSITY

FIGURE 53 FOURIER TRANSFORM OF REDUCED TEST PATTERN

FIGURE 54 FOURIER TRANSFORM OF REDUCED FINE POROSITY

SUMMARY

The experiments described in this report are the concluding efforts of a three year study of the applications of signal processing techniques to nondestructive testing. More than twenty separate experiments have been performed during the program. Each experiment was designed to demonstrate the application of signal processing techniques to a practical NDT problem. The experiments have involved ultrasonic, eddy current, and X-ray inspection. Many of them have been related to problems of aircraft structures. Attention has largely been directed to flaw detection, material property determination and dimensional measurement for metallic and composite materials. The experimental results have indicated that improvements can be made in the sensitivity and ease of application of NDT tests and in the interpretability of the results of these tests by the application of electronic signal processing techniques. The experimental details not presented here have been discussed in earlier reports.[2,3]

In the initial experiments signal averaging was used to detect low amplitude ultrasonic signals. This technique was found to be of practical value in through transmission tests over highly attenuating media. In situations of this kind one encounters low level signals lost in a random noise background, and signal averaging can be very effective in extracting the useful information. Averaging techniques were applied to partially air-coupled, through transmission inspection of honeycomb material and in the development of a dry coupled probe for weak adhesive bond detection. One problem with such methods is the fact that scan rates are reduced if long averaging times are required. It should be noted that the tendency for ultrasonic signals to vary over a wide range of amplitudes frequently makes the application of signal averaging difficult. Many testing situations exist in which the signals are either too large to need processing or too small to be detectable using moderate averaging times.

In another set of experiments various attempts were made to reduce the coherent noise background which is so common in ultrasonic testing. The coherent background is usually caused by surface roughness, grain boundary scattering, and multipath reflections within the test part. This kind of noise is due to real ultrasonic reflections from non-flaw conditions in the part. These signals tend to become confused with reflections from actual flaws and frequently limit the sensitivity of ultrasonic flaw detection systems. Signal averaging was used to reduce the coherent noise background in the ultrasonic detection of inch long tight interface cracks. In this application the averaging essentially served as a low pass filter which removed the high frequency variations due to surface imperfections but retained the weak low frequency signal due to the crack. Coherent background noise was also reduced by performing conventional pulse – echo weld inspection with a narrow moving gate. The use of gates no wider than the ultrasonic pulse to be detected, eliminates a considerable amount of noise. We have shown that it is possible to provide for the automatic variation of the gate time delay in synchronism with the transducer scanning

63

motion. Conventional techniques involve the use of a fixed time delay gate which is wide enough to encompass the effects of transducer motion.

The coherent noise occurring in lamb wave flaw detection was reduced by considering various transducer geometries. The noise background associated with the lamb wave detection of a small drill hole in sheet aluminum was significantly reduced by switching from the conventional pulse echo arrangement to a two transducer arrangement in which the transducers were set at ninety degree angles to one another. Double transducer arrangements were also examined in the ultrasonic shear wave weld inspection geometry. In a number of cases, in which drill holes and EDM slots were used as artificial flaws, a slight reduction in background noise was obtained. It has been found though that in ultrasonic weld inspection it is difficult to determine beforehand the best geometry for a two transducer pitch-catch arrangement. This is because ultrasonic signals are sensitively dependent upon the detailed geometry of flaws. It has been shown that the probability of detecting small flaws is improved by working with an array of transducers in which each transducer is directed towards the same region of the test part. In addition a significant reduction in coherent noise can be obtained by performing cross correlations between the various signals which are made available. It has been shown that a triple product formed between properly chosen signals can improve the signal to noise ratio of a marginally detectable flaw by a factor of five to one.

Some attention has been directed to the problems of recording and display. A technique for recording ultrasonic video information on a low frequency tape recorder was developed. No information is lost as a result of conventional time gating before tape recording. The recording can be played back at an increased rate of speed, at which time one can gate the interesting region of the part and rapidly display the results in C-scan format on a storage oscilloscope. In addition, ultrasonic information has been recorded on a photographic transparency in a C-scan format. A scanning densitometer can be used to produce A-scan recordings from the information recorded on film.

An attempt to use a coherent optical system to improve the clarity of crack indications on an X-ray radiograph was not as successful. Photographic enhancement techniques show more promise. Attempts to quantify weld porosity by observing the fourier transform were hindered by the low contrast and low spatial frequency of the porosity information.

A number of experiments have been performed involving the application of a lock-in amplifier to eddy current inspection. Methods were developed for obtaining quantitative through transmission data. Through transmission thickness measurements were performed and procedures were developed for obtaining a linear relationship between part thickness and eddy current signal. Applications to chemical milling and in-motion thickness measurements were demonstrated. The lock-in amplifier allows through transmission measurements to be made with considerable ease. A phaselock detector and a signal averager were used to measure resistance and inductance changes in conventional eddy current coils. Quantitative data can be automatically collected

and recorded as the eddy current coil scans over the test part. Data of this kind
is normally collected by bridge balance techniques. Balance techniques are cum-
bersome for characterizing the coil reaction to passage over a flaw. The new
technique is useful because it produces quantitative data from the bridge out-of-
balance voltages which one normally records. The authors feel that the use of
quantitative data will aid in the design of new coil shapes and will improve
communication between eddy current investigators. It should be noted that the
same techniques will provide quantitative data for two coil single side probes as
well as for conventional single coil probes.

Finally, correlation techniques have been applied to the reduction of surface
roughness noise in eddy current testing. Eddy current sensitivity to small cracks
is frequently limited by probe liftoff, probe tilt, and surface roughness. Experi-
ments have been performed with an eddy current probe that produces four separate
flaw detection signals. The signals tend to have different background noise
patterns but very similar flaw responses. We have shown that a product of four
signals of this kind significantly reduces surface roughness noise. The multiplica-
tion process is identical to that described earlier in connection with ultrasonic
weld inspection. The use of multi-transducer and multi-coil sensors and the
cross correlation of the signals from these sensors is an interesting area for future
research.

ACKNOWLEDGEMENTS

REFERENCES

1. Nondestructive Testing Handbook, R. C. McMaster, Editor, Vol. II, Section 48, p. 30, Ronald Press, 1959.

2. J. C. Kennedy, W. E. Woodmansee, "Electronic Signal Processing Techniques – Nondestructive Testing, Phase II" – Final Report D180-10589-1, p. 3 and pp. 8-10, November 1970.

3. J. C. Kennedy, W. E. Woodmansee, "Electronic Signal Processing Techniques – Nondestructive Testing, Phase I", – Final Report R-1933, July 1969.

4. J. W. Goodman, "Principles of Fourier Optics", McGraw Hill, 1968.

5. A. R. Shulman, "Optical Data Processing", John Wiley, 1970.

6. A. E. Oaks, "Improved Film Copying Techniques For Increasing Radiographic Contrast and Sensitivity", 1966.